

Altered skeletal muscle mitochondrial biogenesis but improved endurance capacity in trained OPA1-deficient mice

F. Caffin^{1,2}, A. Prola^{1,2}, J. Piquereau^{1,2}, M. Novotova⁴, D. J. David³, A. Garnier^{1,2}, D. Fortin^{1,2}, M. V. Alavi⁵, V. Veksler^{1,2}, R. Ventura-Clapier^{1,2} and F. Joubert^{1,2}

¹INSERM, U-769, Université Paris-Sud F-92296 Châtenay-Malabry, France

²Université Paris-Sud, IFR 141, Châtenay-Malabry, France

³EA3544 Université Paris-Sud F-92296 Châtenay-Malabry, France

⁴Institute of Molecular Physiology and Genetics, Slovak Academy of Sciences, Bratislava, Slovak Republic

⁵Department of Ophthalmology, University of California, San Francisco, USA

Key points

- OPA1 is a mitochondrial protein well known to play a fundamental role in the fusion of the inner membrane, in the organization of mitochondrial cristae and in apoptosis.
- Although the function of mitochondrial dynamics is becoming well understood, its impact on mitochondrial biogenesis is poorly studied, especially in differentiated adult tissues.
- Here we report a novel finding that in fast skeletal muscles OPA1 deletion impairs training-induced mitochondrial biogenesis.
- However, our data reveal that *Opa1*^{+/-} skeletal muscles after training possess better exercise endurance capacity, obviously due to a modification of mitochondrial fatty acid utilization.
- Thus OPA1 deficiency induces a unique pattern of adaptation to endurance training in fast skeletal muscles.

Abstract The role of OPA1, a GTPase dynamin protein mainly involved in the fusion of inner mitochondrial membranes, has been studied in many cell types, but only a few studies have been conducted on adult differentiated tissues such as cardiac or skeletal muscle cells. Yet OPA1 is highly expressed in these cells, and could play different roles, especially in response to an environmental stress like exercise. Endurance exercise increases energy demand in skeletal muscle and repeated activity induces mitochondrial biogenesis and activation of fusion–fission cycles for the synthesis of new mitochondria. But currently no study has clearly shown a link between mitochondrial dynamics and biogenesis. Using a mouse model of haploinsufficiency for the *Opa1* gene (*Opa1*^{+/-}), we therefore studied the impact of OPA1 deficiency on the adaptation ability of fast skeletal muscles to endurance exercise training. Our results show that, surprisingly, *Opa1*^{+/-} mice were able to perform the same physical activity as control mice. However, the adaptation strategies of both strains after training differed: while in control mice mitochondrial biogenesis was increased as expected, in *Opa1*^{+/-} mice this process was blunted. Instead, training in *Opa1*^{+/-} mice led to an increase in endurance capacity, and a specific adaptive response involving a metabolic remodelling towards enhanced fatty acid utilization. In conclusion, OPA1 appears necessary for the normal adaptive response and mitochondrial biogenesis of skeletal

muscle to training. This work opens new perspectives on the role of mitochondrial dynamics in skeletal muscle cells and during adaptation to stress.

(Resubmitted 31 July 2013; accepted after revision 13 September 2013; first published online 16 September 2013)

Corresponding author F. Joubert: U-769 INSERM, Faculté de Pharmacie, Université Paris-Sud, 5 rue J-B Clément, 92296 Châtenay-Malabry, France. Email: frederic.joubert@u-psud.fr

Abbreviations ADOA, autosomal dominant optic atrophy; AK, adenylate kinase; CK, creatine kinase; CS, citrate synthase; DRP1, dynamin-related protein 1; FA, fatty acids; FIS1, fission protein 1; LDH, lactate dehydrogenase; MAS, maximal aerobic speed; MFN, mitofusin; mtDNA, mitochondrial DNA; OPA1, optic atrophy-1; PGC-1, peroxisome proliferator activated receptor gamma co-activator 1; RNA_m, muscle RNA; RT-qPCR, real-time quantitative PCR.

Introduction

In eukaryotic cells, mitochondria are involved in many essential cellular processes. Changes in their viability and function are the cause of severe multi-syndromic diseases. To fulfil their different roles, mitochondria possess dynamic capabilities, fundamental for their biogenesis. Fusion and fission are crucial processes involved in mitochondrial dynamics. The fusion machinery is composed of three large GTPases, the mitofusins (MFN1, MFN2) and the dynamin-related protein OPA1, while fission depends on the GTPase proteins DRP1 and FIS1. Disruption of the mitochondrial balance of fusion–fission, such as a defect in fusion, leads to developmental neurodegenerative diseases in humans (Olichon *et al.* 2006; Chan, 2006). *OPA1* gene mutations have been identified as causing autosomal dominant optic atrophy (ADOA) and are associated with a variety of clinical phenotypes (myopathy, encephalopathy, deafness, etc.) and with mechanisms involving mitochondrial DNA (mtDNA) maintenance disorders (Hudson *et al.* 2008; Amati-Bonneau *et al.* 2008, Yu-Wai-Man *et al.* 2010a).

OPA1 is found in the intermembrane space, on the inner mitochondrial membrane facing the intermembrane space and in the cristae (Olichon *et al.* 2002). It may exist as diverse splice and proteolytic variants (Olichon *et al.* 2002; Suen *et al.* 2008). OPA1 primary function is the fusion of the inner mitochondrial membranes, but it is also involved in additional functions, such as protection against apoptosis through mitochondrial cristae remodelling, control of mtDNA stability and maintenance of mitochondrial respiratory function (Olichon *et al.* 2002; Chen & Chan, 2005; Frezza *et al.* 2006; Elachouri *et al.* 2011; Agier *et al.* 2012). OPA1 deletion in mice is lethal, thus showing the importance of these processes during development.

Understanding of OPA1 function is complicated by the fact that studies on gain and loss of function have led to conflicting results. Mitochondrial fragmentation or elongation has been observed depending on the experimental system (Olichon *et al.* 2003, 2007; Chen *et al.* 2005; Piquereau *et al.* 2012; Agier *et al.* 2012). Interestingly, OPA1 deficiency does not abolish outer membrane fusion but does lead to the possible accumulation of multi-matrix

structures reflecting fusion of the outer membrane without that of the inner mitochondrial membrane, as shown in both the *ex vivo* (Song *et al.* 2009) and *in vivo* (Piquereau *et al.* 2012) setting.

Using a mouse model of haploinsufficiency for the *OPA1* gene, obtained by a deletion of 27 AA in the GTPase domain (Alavi *et al.* 2007, 2009), we previously showed that cardiac mitochondria of *OPA1*^{+/-} mice have altered mitochondrial structure, decreased sensitivity to calcium but normal respiratory function (Piquereau *et al.* 2012). The hearts of *OPA1*^{+/-} mice have normal cardiac function at baseline but develop more serious cardiac hypertrophy and earlier ventricular dysfunction following pressure overload (Piquereau *et al.* 2012). One possible explanation is that the defect in cardiac adaptation could be linked to the abnormal or retarded formation of new mitochondria during adaptive cardiac hypertrophy, due to the involvement of OPA1 in mitochondrial biogenesis.

Mitochondrial biogenesis is a complex process that is defined as the growth and division of pre-existing mitochondria. Correct mitochondrial biogenesis relies on the spatiotemporally coordinated synthesis and import of more than 1000 proteins encoded by the nuclear genome, some of which are assembled with proteins encoded by the mitochondrial DNA within newly synthesized phospholipid membranes of the inner and outer mitochondrial membranes, and finally fission of newly formed mitochondria. All these processes have to be tightly regulated in order to meet the tissue requirements (Ventura-Clapier *et al.* 2008).

To explore in more detail the role of OPA1 in mitochondrial biogenesis, we studied the skeletal muscle adaptations of *OPA1*^{+/-} mice to endurance exercise training. It is well known that under such physiological stress, mitochondrial biogenesis is activated to fulfil the new energetic status of these muscles (Adhihetty *et al.* 2003). We thus hypothesized that OPA1 deficiency may alter the adaptation to exercise endurance training. The results show that *OPA1*^{+/-} mice have the same exercise and training capacity as control mice. After training, *OPA1*^{+/-} mice exhibited altered mitochondrial ultrastructure and biogenesis. Surprisingly, endurance capacity was increased in *OPA1*^{+/-} trained mice. This correlated with a higher

capacity to utilize fatty acid, suggesting a unique adaptive strategy to training.

Methods

Animals

The heterozygous *Opa1*^{329–355del} strain (abbreviated *Opa1*^{+/-}) has been initially described in (Alavi *et al.* 2007). Mice were housed in an environmentally controlled laboratory with a 12 h–12 h light–dark cycle with food and water ad libitum. Investigations were done in accordance with European Community legislation relating to the care and use of animals (Directive 2010/63/EU), and the corresponding French legislation (French decree no. 92–284, June 27, 2007). Experiments were conducted on 6- to 8-month-old male mice. At the end of the experimental period, animals were killed by cervical dislocation. Cardiac, soleus, plantaris, and the white superficial part of gastrocnemius muscles were isolated, washed in ice-cold calcium free Krebs buffer, weighed and rapidly frozen and kept at -80°C , or immediately used to assess mitochondrial function.

Behaviour testing

Tests were conducted on 6-month-old *Opa1*^{+/+} ($n = 12$) and *Opa1*^{+/-} ($n = 12$) male mice. All animals were exposed to a series of behavioural tests designed to assess a range of anxiety-, depression-, stress-related behaviours and agility capabilities. The tests were administered in the following order: open field, elevated plus maze, tail suspension test and rotarod test with a minimum of 3 days between each test. All behavioural testing took place between 10.00 h and 14.00 h. To eliminate odour cues, all testing equipment was thoroughly cleaned after each animal with benzalkonium chloride diluted 100-fold.

The open field protocol. This test has been developed to measure differences in ambulatory activity as a measure of rat emotional reactivity. In addition to information on motor activity, this test can predict anxiolytic activity due to the protocol 'approach-avoidance' created. This test was performed as described previously (Dulawa *et al.* 2004). Motor activity was quantified in four Plexiglas open field boxes measuring $43 \times 43 \text{ cm}^2$ and having a white background (MED Associates, Georgia, VT, USA). Two sets of 16 pulse-modulated infrared photo beams were placed on opposite walls 2.5 cm apart to record x – y ambulatory movements of mice. The test was performed in the dark over a 30 min session; first of all mice were acclimatized to dark for 15 min, then placed in a corner of the boxes. Activity chambers were linked to a computer for data sampling at 100 ms resolution. Computer-defined grid lines divided each open field into centre and surrounding

regions, with each of four lines being 11 cm from each wall. Dependent measures were the number of entries into the various regions of the boxes, the distance travelled in the centre, total time spent in the centre, and distance travelled in the centre divided by total distance travelled. Overall motor activity was quantified as the total distance travelled (cm).

The elevated plus maze test. Anxiety behaviour was measured by the degree of avoidance of the labyrinth's open spaces. The elevated plus maze was performed as previously described (Ramboz *et al.* 1998; Lira *et al.* 2003). The elevated plus maze consisted of a plus-shaped apparatus with two open and two closed arms ($30 \times 6 \text{ cm}$); each with an open roof, elevated about 50 cm from the floor. Testing took place in bright ambient light conditions (800–900 lux). Mice were placed into the central area facing one closed arm and allowed to explore the maze for 5 min. They were recorded by a video camera positioned above the maze and scored by videotracking (Anymaze software, Bioseb, Vitrolles, France). Parameters recorded were: time spent in different parts of the maze and the number of entries in these areas. The total number of entries in all the labyrinth areas was an index of animal locomotion.

The tail suspension test. The tail suspension test is a mouse behavioural test useful in the screening of potential antidepressant drugs, and in assessing of other manipulation that are expected to affect depression related behaviours. The test was performed as previously described (Mayorga *et al.* 2001; David *et al.* 2009). A device was used consisting of six boxes of suspension (Bioseb, Vitrolles, France), which was connected to a computer to quantify the duration of immobility and energy values during agitation. The duration of immobility provides an indicator of the level of resignation. The tails of suspended mice were taped to a hook connected to a vibration sensor; recording duration was 6 min.

The rotarod test. Mouse motor coordination and balance was recorded as previously described (Stemmelin *et al.* 2008; Minasyan *et al.* 2009). The rotarod was composed of a plastic rod 3.2 cm in diameter, 50 cm long, elevated 22.5 cm from the floor, and divided into five compartments, that allows simultaneous testing of five mice. The surface of the rod was lightly roughened to minimize missteps (hind leg slips). Mice were placed on the rod for 3 min at slow rotational speed (4 r.p.m.). Rotational speed gradually accelerated up to 40 r.p.m. If the mouse fell, it got back to its positions on the rod as many times as necessary until the end of the test. The latency to fall from the bar (in seconds) was measured manually and used as an indicator of motor coordination, and the number of

falls as an indicator of their balance. Mice were scored by a highly trained observer blind to the genotype of the mice.

Voluntary wheel running

For voluntary activity, *Opa1*^{+/+} ($n = 21$) and *Opa1*^{+/-} ($n = 20$) animals were housed in individual plexiglas cages (Bionox, Ancy, France) equipped with running wheel and free access to food and water (Momken *et al.* 2004, 2005). The running-wheel system consisted of a 31.8 cm diameter wheel with a 5 cm wide running surface, connected to a direct current (DC) generator allowing slight loading of the wheel (25×10^{-3} N m) at mean maximal speed, with a continuous recording of the output voltage of the DC generator made using a computer for a period of 8 weeks. Instantaneous speed, calculated from the voltage and the resistive load on the DC generator, enabled calculation of the daily running distance. All daily parameters were averaged over each week for each animal.

Forced treadmill activity

Prior to the experiments, all mice were acclimatized to the rodent treadmill and running exercise by 12 min activity in the treadmill apparatus (Habouzit *et al.* 2009), 4 days before the day of the experiment (D-4; running for 2 min at 10 m min⁻¹, 4 min at 13 m min⁻¹, 2 min at 15 m min⁻¹, 2 min at 16.5 m min⁻¹ and 2 min at 18 m min⁻¹ at a 4% slope), and 3 days before the day of the experiment (D-3; running for 2 min at 13 m min⁻¹, 2 min at 16 m min⁻¹, 2 min at 18 m min⁻¹, 4 min at 20 m min⁻¹ and 2 min at 22 m min⁻¹ at a 4% slope). Compressed air, triggered by a photocell at the end of each lane, was used, if necessary, to maintain the running motivation during acclimatization and experiments.

On the day of the experiment (D+0), to measure the maximal aerobic running performance, all animals were briefly warmed up by running 10 m min⁻¹ for 6 min. Then animals were exercised until they were no longer able to maintain the increasing speed of the treadmill. Treadmill speed was increased by 3.3 m min⁻¹ every 1.5 min to reach 30 m min⁻¹ at a 4% slope, and then treadmill speed was increased by 3.3 m min⁻¹ every min at a 4% slope. This allowed the maximal aerobic speed (MAS) to be determined for each animal.

Exercised animals were rested for 48 h before the second experiment (i.e. on D+2) involving exhaustive running exercise. To measure the maximal endurance performance, each animal was briefly warmed up by running 10 m min⁻¹ for 6 min at a 4% slope. Then, treadmill speed was slowly increased during a period of 6 min until it reached 60% of MAS for a 4% slope for each animal. After warming up, animals were exercised at 60% of their MAS until exhaustion. Sedentary *Opa1*^{+/+} ($n = 16$), *Opa1*^{+/-} ($n = 15$), and trained *Opa1*^{+/+} ($n = 9$) and *Opa1*^{+/-} ($n = 7$) mice were used.

Enzyme assay

Complete enzyme extractions from small pieces of frozen tissues were done in an ice-cold buffer (50 mg ml⁻¹; containing (in mM): Hepes 5 (pH 8.7), EGTA 1, DTT 1, and 0.1% Triton X-100) using a Bertin Pre-cellys 24 homogenizer (Bertin, Montigny-le-Bretonneux, France). Protein concentration was assessed using the bicinchoninic acid assay. Total activities of cytochrome oxidase (COX), citrate synthase (CS), creatine kinase (CK), adenylate kinase (AK), β -hydroxyacyl-CoA dehydrogenase (HADHA) and LDH were assayed (30°C, pH 7.5) using standard spectrophotometric assays. Activities were given as $\mu\text{mol min}^{-1}(\text{g protein})^{-1}$ ($\mu\text{mol min}^{-1}$, international units, IU). CK isoenzymes were separated using agarose (1%) gel electrophoresis performed at 250 V for 90 min. Individual isoenzymes were resolved by incubation of the gels with a coupled enzyme system (Momken *et al.* 2005).

Western blot experiments

Protein extracts (50 μg) from white gastrocnemius muscle of 8-month-old *Opa1*^{+/+} and *Opa1*^{+/-} mice were loaded on 10% sodium dodecyl sulfate polyacrylamide gels, separated for 120 min at 150 V and subsequently transferred to Hybond nitrocellulose membranes (Amersham) using a Bio-Rad blot system for 90 min at 150 V. Thereafter, blots were blocked for 60 min in 5% milk in phosphate buffered saline and Tween at room temperature, followed by incubation with different primary antibodies (OPA1: BD Biosciences, San Jose, California, USA 612606, CS: Abcam, Cambridge, MA, USA 96600, GAPDH: Cell Signaling, Danvers, MA, USA 2118, Oxphos Complexes: MitoSciences, Eugene, Oregon, USA 604, CPT1, Santa Cruz, Dallas, Texas, USA 139482, CPT2: personal gift from Carina Pripp-Buus, Institut Cochin, Paris) overnight at 4°C. After washing, the membranes were incubated with the appropriate secondary antibodies for 60 min at room temperature and revealed using a chemiluminescent substrate (Immobilion Western HRP, Millipore). Light emission was recorded using a chemiluminescent detection system (ChemiDoc XRS; Bio-Rad) and quantified by image-analysis software (Quantity One Bio-Rad). Protein content was normalized to GAPDH or β -actin (markers of cytoplasm) or to CS (a marker of mitochondria).

Mitochondrial (mtDNA) and nuclear (nDNA) DNA content

Total DNA was extracted from white gastrocnemius. Briefly, muscles were minced in 500 μl of buffer 1 (TrisHCl 10 mM, NaCl 10 mM, EDTA 25 mM, SDS 1%, proteinase K 0.4 mg ml⁻¹, pH 7.5) with cleaned scissors

and incubated overnight at 37°C. After addition of 50 μl of saturated NaCl solution, the homogenates were centrifuged at 500 g for 15 min. Isopropanol (50 μl) was added to supernatants which were then incubated for 45 min at -20°C . After a centrifugation at 16000 g for 20 min, the pellets were kept, washed with ethanol 70%, resuspended in buffer 2 and finally warmed at 70°C. mtDNA content was measured by real-time quantitative PCR (RT-qPCR) using SYBR[®]Green technology with specific primers for a mitochondrial sequence (Dloop, forward primer ATAGCCGTCAAGGCATGAAA, reverse primer GATTGGGTTTTGCGGACTAA) and for a nuclear gene (B2M (beta-2-microglobulin), forward primer TGGTAAAGCAAAGAGGCCTAA, reverse primer AGAAGTAGCCACAGGGTTGG). The difference between the threshold cycle (Ct) of nuclear gene and mtDNA sequence (ΔCt) was used to assess the mtDNA/nDNA ratio, which was calculated using the following formula: $2(2 - \Delta\text{Ct})$ (for details see Dimmock *et al.* 2010).

Mitochondrial respiration

Respiratory parameters of total mitochondrial population were studied *in situ* as previously described (Kuznetsov *et al.* 2008). Fibres of plantaris and white gastrocnemius muscles were separated under a binocular microscope in skinning (S) solution (below) at 4°C, and permeabilized in the same solution with 50 $\mu\text{g ml}^{-1}$ of saponin for 30 min. Then, adenine nucleotides and creatine phosphate were eliminated by 10 min washing in respiration (R) solution (below) at 4°C. Experiments were performed on washed fibres under continuous stirring in an oxygraphic cell (Strathkelvin Instruments, UK), equipped with a Clark electrode, containing 3 ml of solution R with additional substrates at 22°C. After the experiments, fibres were collected and dried. Respiration rates were expressed as $\mu\text{mol O}_2 \text{ min}^{-1} (\text{g dry weight})^{-1}$.

Solutions S and R both contained (in mM): EGTA–CaEGTA buffer 10 (free Ca^{2+} concentration 100 nM), free Mg^{2+} 1, taurine 20, DTT 0.5, and imidazole 20 (pH 7.1). Ionic strength was adjusted to 160 mM by addition of $\text{CH}_3\text{KO}_3\text{S}$. Solution S also contained MgATP 5 and PCr 15, whereas solution R contained 3 mM KH_2PO_4 and 2 mg ml^{-1} fatty acid-free BSA.

The experimental protocol used was based on substrate utilization pathways. Firstly basal mitochondrial respiration rate was determined using 2 mM ADP and 5 mM malate (V_0). Secondly fatty acid oxidation rate was determined using palmitoyl-coenzyme A + carnitine (100 μM + 2 mM), followed by the measurement of respiration rate with pyruvate (1 mM). Lastly to determine the maximal capacity of the respiratory chain (complexes I, II, III, IV), glutamate (10 mM) and succinate (15 mM) were added to maximally activate complex I and II (V_{max}). Fatty acid utilization was calculated by subtracting V_0

from the fatty acid oxidation rate. Fatty acid utilization was expressed as a percentage of V_{max} .

Electron microscopy

Samples of the white gastrocnemius muscles from 8-month-old mice were prepared for electron microscopy as previously described in (Novotova *et al.* 2006). Isolated muscles were stretched by 30% of their resting length in nominally calcium-free Krebs solution, and fixed with 2% glutaraldehyde in cacodylate buffer (150 mM sodium cacodylate, 2.0 mM CaCl_2 ; pH 7.3) for 30 min. Four samples of each muscle were dissected from superficial regions around the central part of the muscle and fixed again for 45 min with 2% glutaraldehyde in cacodylate buffer, post-fixed for 45 min with 1% OsO_4 in cacodylate buffer, and contrasted overnight with a saturated solution of uranyl acetate in H_2O . The samples were embedded in Durcupan (Fluka AG, Switzerland). Ultrathin (58–60 nm) longitudinal or transversal sections, were cut by Powere-Tome MT-XL ultramicrotome (RMC/Sorvall, Tucson, USA), placed on copper grids covered with formvar, and contrasted by lead citrate. The sections were examined with JEM 1200 electron microscope (Jeol, Japan). Images were recorded using a Gatan Dual Vision 300W CCD camera (Gatan Inc., USA).

EM quantification of individual mitochondrial surface in *Opa1*^{+/+} and *Opa1*^{+/-} white gastrocnemius muscles was performed using Image J software on 18 slices (randomly chosen, magnification 50,000 \times) per animal (5 different animals for trained and 2 for sedentary animals) as previously (Piquereau *et al.* 2012). The mean value of individual mitochondrial surface was obtained on the whole population of mitochondria (for each group), and the distribution of these mitochondrial surfaces calculated for each animal in each group.

RT-qPCR analysis

Total muscle RNA (RNA_m) was extracted from 10 mg frozen tissue samples using a standard procedure with Bertin Precellys 24 and ice-cold Trizol reagent (Invitrogen) for extraction. Then, RNA_m was precipitated by ethanol and resuspended in RNase-free water. RNA was quantified and checked for purity using the ratio of its absorbance at 260 and 280 nm. Oligo-dT first strand complementary DNA was synthesized from 1 μg total RNA according to the protocol provided with the iScript cDNA synthesis kit (Bio-Rad).

Quantification of mRNA via production of cDNA was assessed using the SYBR Green method as previously described (Piquereau *et al.* 2010) on a CFX96 (Bio-Rad).

Each PCR amplification was performed with 12.5 ng of cDNA in a total reaction volume of 15 μl . The reaction

mixtures consisted of 5 μl diluted template, 3 μl Master Mix (Roche) and 0.75 μM forward and reverse primers (Table 1). After 10 min of *Taq* polymerase activation, amplification was allowed to proceed for 45 cycles: each cycle consisting of denaturation at 95°C for 10 s, annealing at specific temperature (Table 1) for 5 s and extension at 72°C for 7 s. Quantification of test sample concentration was assessed using the SYBR Green method on a Light-Cycler rapid thermal cycler (Roche Diagnostics) and was achieved using a linear standard curve constructed from the analysis of a fivefold serial dilution from cDNA of sedentary *Opa1*^{+/+}. Primers were designed to be specific for a different exon of the target gene sequence, thereby eliminating the possibility of amplifying genomic DNA; primer sequences are presented in Table 1. A basic local alignment search tool (BLAST) search performed for each set of primers revealed that sequence homology was obtained only for the target gene. HK2 was chosen as housekeeping gene as its expression did not differ between groups.

Statistics analysis

All data are presented as means \pm SEM, and significance was set at $P < 0.05$. Two-way ANOVA was used to study the global effect of training activity and OPA1 genotype, followed by Newman–Keuls *post hoc* test when appropriate to determine individual differences. For voluntary activity measurements, paired Student's *t* test was applied. * indicates *Opa1*^{+/−} versus *Opa1*^{+/+}, # indicates active versus sedentary, \$ indicates global effect of genotype or training.

Results

Characterization of sedentary *Opa1*^{+/−} mice

Sedentary *Opa1*^{+/−} mice evidenced a slight but highly significant lower body and heart weight compared to their control littermates (Table 2). Before starting training experiments, we checked to see that the ubiquitous mutation of OPA1 had no impact on global mice behaviour, which could influence the results of the running wheel experiments. Six-month-old *Opa1*^{+/+} and *Opa1*^{+/−} male mice were therefore exposed to a series of behavioural tests that ranged in stress in order to estimate their stress resistance, degree of anxiety and agility (Fig. 1). No difference was observed in any parameters during the open field test (Fig. 1A and B) and in the elevated plus maze test (Fig. 1C, D and E). Furthermore, in the tail suspension test, both strains had the same period of immobility-enduring discomfort (Fig. 1F). Finally, motor coordination and balance capabilities of the mice were estimated using an accelerod. Again, no difference was observed between the two mouse strains (Fig. 1G). Thus,

we concluded that OPA1 deficiency has no major impact on mouse behaviour.

Additional experiments were also performed to verify that mutant mice possessed the same capacity to exercise at basal level. Therefore, animals were tested for their MAS and their endurance by forced treadmill activity (Fig. 2A). Both groups reached the same maximal aerobic velocity and had the same endurance time. No difference was also observed at the metabolic level since circulating glucose, cholesterol and triglycerides measured in blood samples taken before and after exhaustion was reached were identical (data not shown). We therefore concluded that sedentary *Opa1*^{+/−} mice had no major behavioural disorder and possessed the same physical aerobic capacity as control mice.

Response of *Opa1*^{+/−} mice to training

The impact of OPA1 mutation on mouse voluntary exercise was estimated by monitoring the weekly averaged running distance of *Opa1*^{+/+} and *Opa1*^{+/−} mice and the maximal speed reached in the wheel (Fig. 2B). In both groups, we observed a progressive increase in these parameters with time, with no significant difference between animals. Only small differences were observed for the maximal speed at weeks 2, 3 and 6, but globally OPA1 deficiency did not alter the ability of the mice to perform voluntary running activity and to train.

Although both groups of animals seemed to be able to perform the same physical activity, it was possible that their endurance capacity differed after prolonged training. Thus, we measured the maximal running capacity and running time before exhaustion in 8-month-old animals using the same forced treadmill test at the end of the training period on (Fig. 2A). As expected, training improved these parameters in both groups due to its beneficial effect on the physical capacity of animals. But, surprisingly, the endurance capacity of *Opa1*^{+/−} mice increased five times after training and much more than for *Opa1*^{+/+} mice (two-fold increase, $P < 0.01$; Fig. 2A, right panel) with a strong genotype effect ($P < 0.001$). Thus, after training, *Opa1*^{+/−} mice became better adapted to forced exercise than control mice.

Data given in Table 2 show the effect of OPA1 mutation and training on anatomical parameters of sedentary and trained mice. Eight-month-old *Opa1*^{+/−} mice had lower body weights and body weight-to-tibia lengths compared to *Opa1*^{+/+} mice. When normalized to body weight, no difference was observed in organ weights between sedentary mice. After training, body weight was not changed. Left ventricular weight hypertrophy was only observed in *Opa1*^{+/−} mice, while soleus hypertrophy occurred in both groups of animals (training effect $P < 0.001$). No effect of training was observed on plantaris muscle weight. Thus, the main anatomical effect of OPA1

Table 1. Primers and conditions for real-time PCR amplification

Genes	GeneBank No.	Forward primers (5'>3') Reverse primers (5'>3')	PCR product size (pb)	Annealing temperature (°C)
ACADM	NM_007382	CCG TTC CCT CTC ATC AAA AG ACA CCC ATA CGC CAA CTC TT	129	60
CD36	NM_007643	CCA CTG TGT ACA GAC AGT TTT GG GCT CAA AGA TGG CTC CAT TG	195	60
CPT1 β	NM_009948	TCA CCT GGG CTA CAC GGA GA TCG GGG CTG GTC CTA CAC TT	219	65
COX I	NC_006914	CAC TAA TAA TCG GAG CCC CA TTC ATC CTG TTC CTG CTC CT	129	60
COX IV	NM_017202	TGG GAG TGT TGT GAA GAG TGA GCA GTG AAG CCG ATG AAG AAC	273	58
CS	NM_130755	CAA GAT TGT GCC CAA TAT CCT C TTC ATC TCC GTC ATG CCA TA	111	60
DRP1	NM_053655	CTG ACG CTT GTG GAT TTA CC CCC TTC CCA TCA ATA CAT CC	277	58
ERR α	NM_001008511	TCA AGG AGG GTG TGC GTC TG CTT GGC CCA GCT GAT GGT GA	296	65
FIS1	NM_025562	GCC TGG TTC GAA GCA AAT AC CAC GGC CAG GTA GAA GAC AT	116	60
GLUT4	NM_009204	CCG TGG CCT CCT ATG AGA TAC T AGG CAC CCC GAA GAT GAG T	122	64
HADHA	NM_178878	GTA TCT TCG CCA GCA ACA CA ACC ACA ATG ATG ACC TTC CC	208	60
HK2	NM_013820	TTT CAC CTT CTC GTT CCC CT GTC ATT CAC CAC AGC CAC AA	175	60
MCIP1	NM_019466	CAG CGA AAG TGA GAC CAG GG ACG GGG GTG GCA TCT TCT AC	309	60
MFN1	NM_024200	TGC CCT CTT GAG AGA TGA CC AGA GCC GCT CAT TCA CCT TA	182	60
MFN2	NM_133201	GGG GCC TAC ATC CAA GAG AG CCT TGG ACA GGT ACC CTT TG	115	60
NRF1	NM_010938	TTA CTC TGC TGT GGC TGA TGG CCT CTG ATG CTT GCG TCG TCT	92	60
OPA1	NM_133752	TCA GCA AAG CTT ACA TGC AGA TGC TTG GAC TGG CTA CAT TTT	180	60
PDK4	NM_013743	CCT TCA CAC CTT CAC CAC AT AAA GAG GCG GTC AGT AAT CC	189	60
PGC1 α	NM_008904	CAC CAA ACC CAC AGA GAA CAG GCA GTT CCA GAG AGT TCC ACA	210	58
PPAR α	NM_011144	AAG TGC CTG TCT GTC GGG AT GCT TCG TGG ATT CTC TTG CC	161	62
PPAR $\beta\delta$	NM_011145	GCC TCC ATC GTC AAC AAA GA TCT ACC TGG GGC ACA TTC AT	230	60
Tfam	NM_009360	GCT GAT GGG TAT GGA GAA G GAG CCG AAT CAT CCT TTG C	161	56

ACADM, acyl-coenzyme A dehydrogenase medium chain; CD36, cluster of differentiation 36; CPT1 β , muscle isoform of carnitine palmitoyl transferase I; COX I, cytochrome c oxidase subunit I; COX IV, cytochrome c oxidase subunit IV; CS, citrate synthase; DRP1, dynamin-1-like protein; ERR α , estrogen related receptor alpha; FIS1, mitochondrial fission 1 protein; GLUT4, glucose transporter type 4; HADHA, hydroxyacyl-coenzyme A dehydrogenase subunit alpha; HK2, hexokinase 2; MCIP1, regulator of calcineurin 1; MFN, 1 and 2 mitofusin 1 and 2; NRF1, nuclear respiratory factor 1; OPA1, optic atrophy type 1; PDK, pyruvate dehydrogenase kinase; PGC, peroxisome proliferator activated receptor gamma co-activator; PPAR α and $\beta\delta$, peroxisome proliferator-activated receptor α and $\beta\delta$; Tfam, mitochondrial transcription factor A.

Table 2. Anatomical data

	Sedentary		Trained		Genotype	Training	Interaction
	<i>Opa1</i> ^{+/+}	<i>Opa1</i> ^{+/-}	<i>Opa1</i> ^{+/+}	<i>Opa1</i> ^{+/-}			
BW (g)	33.6 ± 0.6	29.7 ± 0.4***	32.5 ± 0.9	30.0 ± 0.5*	\$\$\$	n.s.	n.s.
HW (mg)	178.9 ± 7.5	154.1 ± 6.1*	178.1 ± 5.6	169.9 ± 5.0	\$\$	n.s.	n.s.
LVW (mg)	111.5 ± 4.9	95.4 ± 1.6**	113.3 ± 3.5	107.2 ± 2.4#	\$\$	n.s.	n.s.
Soleus W (mg)	9.9 ± 0.3	9.1 ± 0.3	12.2 ± 0.4###	10.9 ± 0.5*##	\$\$	\$\$\$	n.s.
Plantaris W (mg)	21.3 ± 0.9	21.8 ± 1.1	22.1 ± 1.1	19.9 ± 1.2	n.s.	n.s.	n.s.
Tibia length (cm)	1.80 ± 0.01	1.81 ± 0.01	1.80 ± 0.01	1.79 ± 0.01	n.s.	n.s.	n.s.
BW/TL (g cm ⁻¹)	18.7 ± 0.2	16.4 ± 0.2***	18.0 ± 0.4	16.8 ± 0.2**	\$\$\$	n.s.	n.s.
HW/BW (mg g ⁻¹)	5.3 ± 0.2	5.2 ± 0.2	5.5 ± 0.2	5.7 ± 0.2	n.s.	n.s.	n.s.
LVW/BW (mg g ⁻¹)	3.34 ± 0.17	3.18 ± 0.07	3.5 ± 0.09	3.57 ± 0.07#	n.s.	\$\$	n.s.
SW/BW (mg g ⁻¹)	0.30 ± 0.01	0.29 ± 0.01	0.38 ± 0.01###	0.36 ± 0.02###	n.s.	\$\$\$	n.s.
PW/BW (mg g ⁻¹)	0.63 ± 0.03	0.72 ± 0.03	0.68 ± 0.04	0.67 ± 0.04	n.s.	n.s.	n.s.

BW, body weight; HW, heart weight; LVW, left ventricular weight; SW, soleus weight; PW, plantaris weight; TL, tibia length. Sedentary *Opa1*^{+/+} (*n* = 17), *Opa1*^{+/-} (*n* = 16); trained *Opa1*^{+/+} (*n* = 19), *Opa1*^{+/-} (*n* = 17) 8-month-old mice. Values are means ± SEM. Significant differences: *,\$P < 0.05, **,\$\$P < 0.01, **,\$\$\$P < 0.001, * = *Opa1*^{+/-} versus *Opa1*^{+/+}, # = active versus sedentary, \$ = global effect of genotype or training.

deficiency in response to exercise was cardiac hypertrophy, which may reflect an adaptation of *Opa1*^{+/-} mice to sustained voluntary exercise.

Mitochondrial adaptation of trained *Opa1*^{+/-} skeletal muscle

Exercise training is expected to increase mitochondrial biogenesis. We first measured the level of OPA1 protein in the four groups of animals (Fig. 3A). White gastrocnemius muscle was used for this purpose. Results showed that *Opa1*^{+/-} mouse skeletal muscle had a 50% reduction of OPA1 protein, as expected, with no change in protein variants. After training, OPA1 protein content was significantly increased in *Opa1*^{+/+} mice, but not in *Opa1*^{+/-} mice. CS protein content, a marker of mitochondrial mass, was also increased after training, but to a lower extent in *Opa1*^{+/-} mice compared to *Opa1*^{+/+} mice. These results revealed possible alteration of mitochondrial biogenesis in *Opa1*^{+/-} mice. We thus studied in more detail mitochondrial biogenesis and function in order to understand how *Opa1*^{+/-} mice adapt to exercise training.

Citrate synthase (CS) and cytochrome oxidase (COX) activities were measured to further assess muscle mitochondrial mass before and after training (Fig. 4A). OPA1 haploinsufficiency did not alter these activities in the basal state, nor after training, in oxidative muscles (ventricle and soleus). By contrast, in fast skeletal muscles (plantaris and white gastrocnemius) of both mouse strains, training induced an increase in CS and COX activities. This increase was, however, blunted

in *Opa1*^{+/-} mice, again suggesting possible alteration of mitochondrial biogenesis in response to training. The same behaviour was observed for mitochondrial complexes in the white gastrocnemius muscle (Fig. 4B). Finally, we assessed mtDNA/nDNA content (Fig. 3C). Measurements revealed a slight decrease in sedentary *Opa1*^{+/-} animals compared to *Opa1*^{+/+} mice and a significant increase after training only in the *Opa1*^{+/+} mice.

To understand at which step mitochondrial biogenesis was disturbed in *Opa1*^{+/-} mice, we next measured the expression of genes involved in mitochondrial dynamics and biogenesis in white gastrocnemius muscle (Fig. 5A). In sedentary animals, none of the mRNA levels of genes involved in mitochondrial dynamic were modified, showing no clear compensation for OPA1 deficiency. Exercise training clearly activated the transcription cascade of mitochondrial biogenesis, including the genes involved in mitochondrial dynamics, with OPA1 similarly activated in both mouse strains. A training effect was observed for all genes except for MCIP1, the marker of calcineurin activation and Tfam, while a genotype effect was observed only for PGC-1 α . Interestingly, in this glycolytic muscle a large induction of mRNA levels was observed after training for all the genes involved in fatty acid and carbohydrate utilization (Fig. 5B) except for PDK4, but again without significant differences between strains except for HADHA and PDK4. In conclusion, OPA1 deficiency had no major impact on the response to exercise training at the transcription level of genes involved in mitochondrial dynamics, biogenesis, and substrate utilization.

Mitochondrial morphology of *Opa1*^{+/-} skeletal muscle

Because OPA1 deficiency can affect mitochondrial morphology, we also studied the mitochondrial network organization in the white gastrocnemius of the four groups of animals (Fig. 6). Muscle fibres of control *Opa1*^{+/+}

mice displayed typical ultrastructural features of fast glycolytic fibres. Myofibrils were arranged in register, with triads present near the I- and A-band boundaries. Profiles of mitochondria in longitudinal sections were small, with mitochondria localized at the sides of the I-bands near the Z-lines. Ultrastructural analysis of the control fibres revealed the presence of tubular aggregates

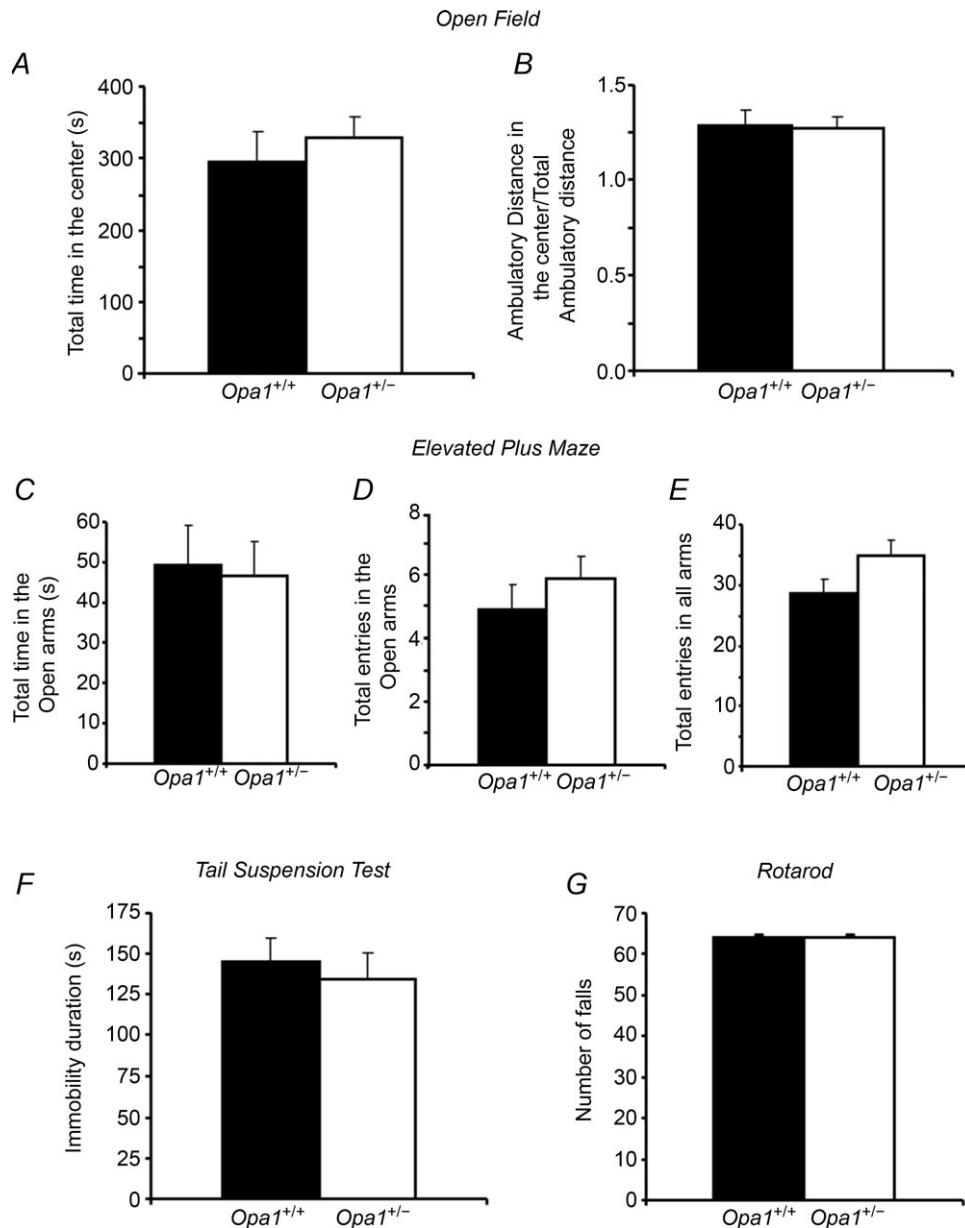


Figure 1. Similar behaviour of *Opa1*^{+/+} and *Opa1*^{+/-} mice

A and B, effects of OPA1 deficiency on anxiety behaviours in the open field test. Anxiety is measured as mean of the total time spent in the centre in seconds (A). Locomotor activity is measured as total ambulatory distance travelled (B). C–E, effects of OPA1 deficiency on anxiety behaviours in the elevated plus maze. Anxiety is expressed as mean total time in the open arms (C), as mean total entries in the open arms (D) and as mean total entries in all arms as an index of their locomotion (E). F, effects of OPA1 deficiency on behaviour in the tail suspension test. Results are expressed as mean of immobility duration (in seconds) as their resignation indices. G, effects of OPA1 deficiency in the rotarod test. The number of falls during accelerating rotarod test as balance capabilities indicator. Values are means \pm SEM. Sedentary *Opa1*^{+/+} ($n = 12$) and *Opa1*^{+/-} ($n = 12$) 6-month-old animals.

intercalated between myofibrils and under the sarcolemma. Mitochondrial ultrastructure was normal with a regular arrangement of cristae and a homogeneous matrix (Fig. 6A). In *Opa1*^{+/-} mice, the ultrastructure of muscle fibres was slightly disordered in some regions of the fibres due to an irregular arrangement of the sarcomeres. Electron microscopic analysis revealed regions with regularly arranged mitochondria near the Z-lines but the size of mitochondria appeared heterogeneous compared to the control. Some mitochondria were devoid of cristae

and matrix (Fig. 6B and D), and signs of mitochondrial destruction were often observed (Fig. 6C and D). A specific feature of muscle fibres of *Opa1*^{+/-} mice was the presence of large mitochondria. The ultrastructure of giant mitochondria was modified. Disappearance of cristae in these mitochondria was accompanied by formation of irregular vacuoles (Fig. 6E). In some large mitochondria, altered cristae morphology, as well as the absence of outer mitochondrial membranes was found (Fig. 6F).

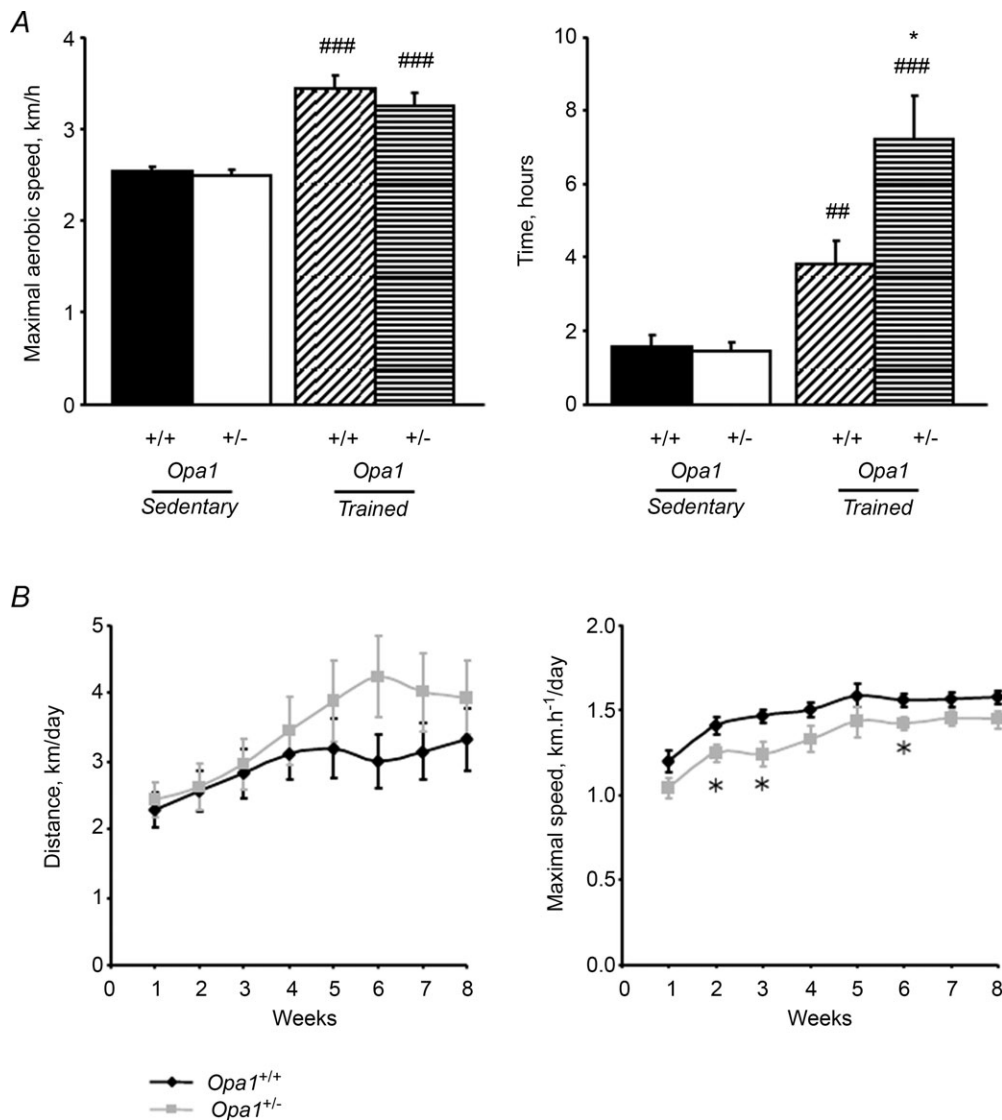


Figure 2. Similar training capacity of *Opa1*^{+/+} and *Opa1*^{+/-} mice but increased endurance performance in trained *Opa1*^{+/-} mice

A, forced activity of 6-month-old or after 2 months of training *Opa1*^{+/-} and *Opa1*^{+/+} animals expressed as means of maximal running speed (left panel) or running time before exhaustion (right panel). Values are means \pm SEM. Significantly different: * $P < 0.05$, ## $P < 0.01$, ### $P < 0.001$. * = *Opa1*^{+/-} versus *Opa1*^{+/+}, # = active versus sedentary. Sedentary *Opa1*^{+/+} ($n = 16$), *Opa1*^{+/-} ($n = 15$), trained *Opa1*^{+/+} ($n = 9$) and *Opa1*^{+/-} ($n = 7$) mice. B, voluntary wheel running capacity of *Opa1*^{+/+} ($n = 21$) and *Opa1*^{+/-} ($n = 20$) 6-month-old animals expressed as daily running distance (left panel) or maximal running speed (right panel) over a 8 week period. Values are means \pm SEM. *Significantly different from *Opa1*^{+/+}, $P < 0.05$.

Quantitative analysis of EM images was performed, with results presented in Fig. 6G, confirming that, in sedentary and trained animals, mitochondria from *Opa1*^{+/-} mice were larger than those of control mice. Interestingly, training seemed to induce an increase in mitochondrial size in both mouse strains, which was more pronounced in *Opa1*^{+/-} mice. Distribution of mitochondrial sizes confirmed the appearance of large mitochondria after training in both mice, which was more pronounced in *Opa1*^{+/-} mice. The irregular size of mitochondria in *Opa1*^{+/-} trained mice compared to wild type was evidenced by an increase of the standard deviation of mitochondrial surface (0.035 ± 0.005 for trained *Opa1*^{+/+} and 0.052 ± 0.006 for trained *Opa1*^{+/-}, $P < 0.05$).

Effect of training on energy metabolism in *Opa1*^{+/-} mice

Since the lack of OPA1 could influence the response to training of enzymes involved in energy transfer, we measured creatine kinase (CK), adenylate kinase (AK)

and lactate dehydrogenase (LDH) activities in the four groups of animals (Table 3). Globally, neither physical activity nor OPA1 deficiency induced major changes in the activities of these enzymes. Interestingly, however, the training-induced increase in activity in plantaris MM-CK and MB-CK isoforms of CK (mi-CK) was three times lower in *Opa1*^{+/-} mice than in *Opa1*^{+/+} mice, consistent with the observation of blunted mitochondrial biogenesis, while LDH activity was slightly decreased in the soleus of *Opa1*^{+/-} trained mice. Thus, genotype did not appear to have significant effects on intracellular energy transfer, which could explain how the two groups of animals could achieve the same training performances.

Finally, the activity of the respiratory chain and the ability of mitochondria to utilize different substrates were studied in fast and mixed skeletal muscles by measuring oxygen consumption before and after training (Table 4). In control mice, training did not improve maximal respiratory capacities of either plantaris or white gastrocnemius muscles (Table 4). *Opa1*^{+/-} trained mice showed

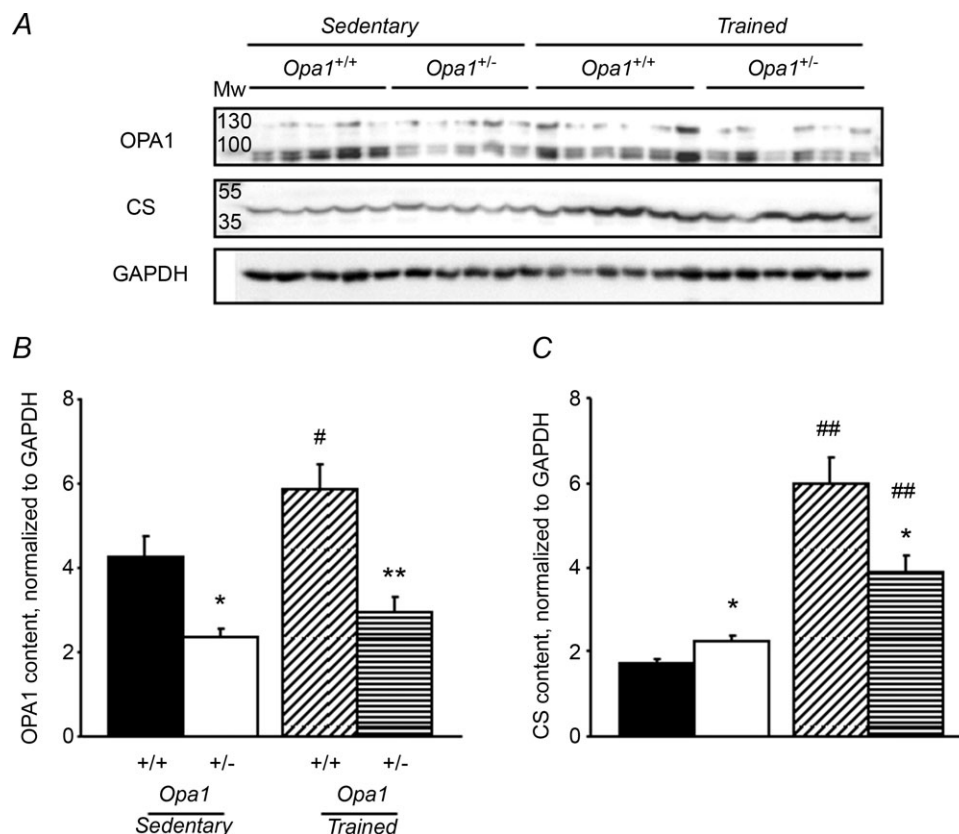


Figure 3. Decreased expression of mitochondrial proteins following training in *Opa1*^{+/-} mice

A, original recording of OPA1 and CS protein content. GAPDH was used for normalization. Each lane was loaded with 50 μ g of total white gastrocnemius muscle extracts of 8-month-old sedentary or active *Opa1*^{+/+} and *Opa1*^{+/-} mice. B, OPA1 content normalized to GAPDH. C, CS content normalized to GAPDH. Values are means \pm SEM. Significant differences: # $P < 0.05$, ## $P < 0.01$ trained versus sedentary, * $P < 0.05$, ** $P < 0.01$ *Opa1*^{+/-} versus *Opa1*^{+/+} for sedentary or trained mice. Sedentary *Opa1*^{+/+} ($n = 5$), *Opa1*^{+/-} ($n = 5$), trained *Opa1*^{+/+} ($n = 6$) and *Opa1*^{+/-} ($n = 6$) 8-month-old mice.

an increase in V_{\max} (+46%) only in plantaris muscle. Fatty acid (FA) utilization, a relevant marker of endurance capacity, was also estimated in the plantaris and white gastrocnemius muscles (Fig. 7A). Interestingly, training had no effect on FA utilization in control mice, but had a significant effect on $Opa1^{+/-}$ trained mice, FA utilization was improved by 47% in plantaris muscle and by 57% in white gastrocnemius muscle. Interaction

between genotype and training effects were observed for several parameters relating to FA utilization. No change in pyruvate utilization was observed in plantaris and white gastrocnemius (Table 4). All the results suggest that a training-induced metabolic remodelling occurred in $Opa1^{+/-}$ mice, suggesting a better ability to utilize FA, which could explain the better endurance capacity of $Opa1^{+/-}$ mice after training.

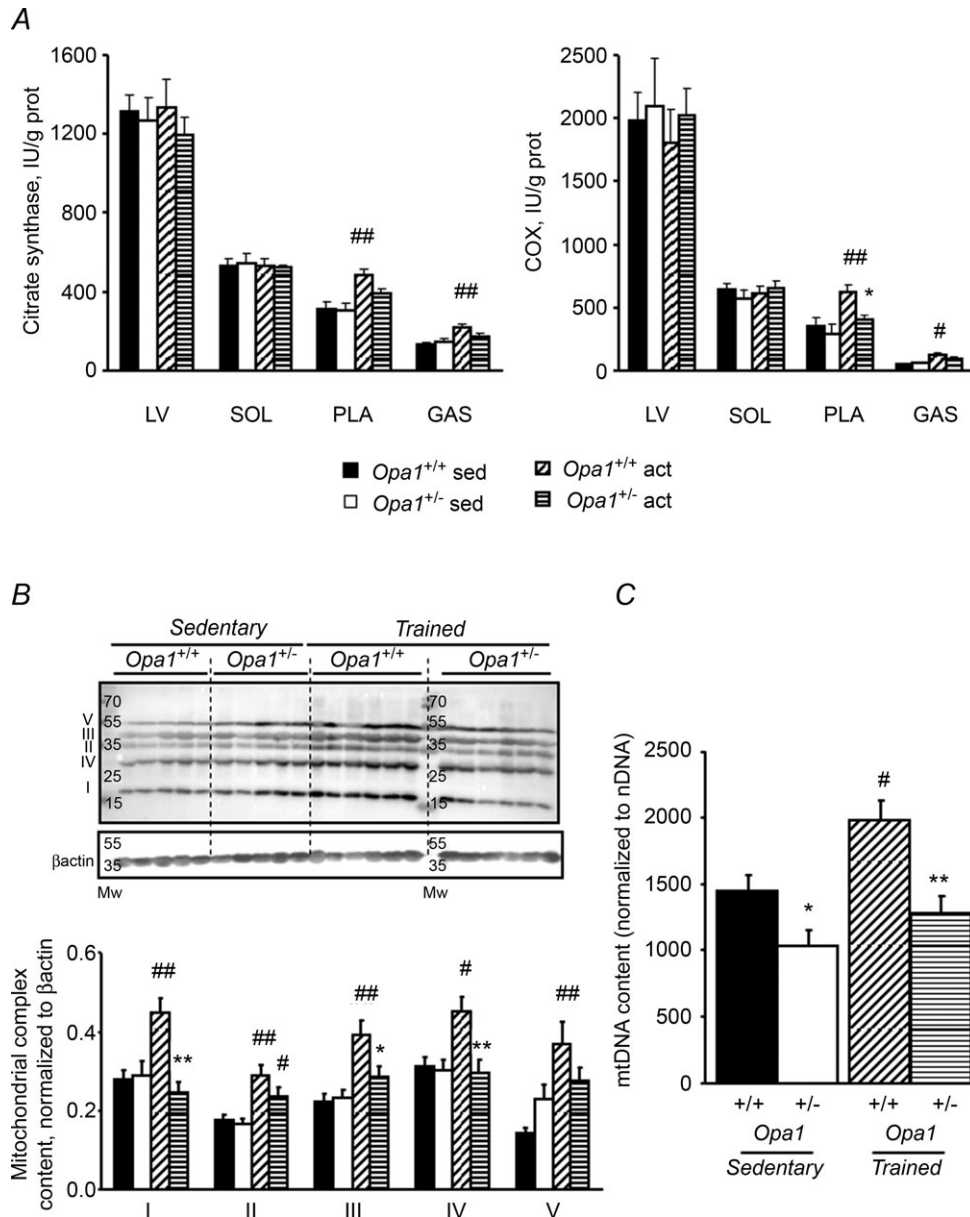


Figure 4. Mitochondrial protein and mtDNA content following training in $Opa1^{+/-}$ mice

A, citrate synthase (CS) and cytochrome oxidase (COX) activities. Activities were measured spectrophotometrically in left ventricle (LV), soleus (SOL), plantaris (PLA) and white gastrocnemius (GAS) muscles of sedentary and trained mice. B, original recording of subunits of mitochondrial complexes in GAS (upper lane). Proteins were normalized to β -actin (lower lane). C, ratio of mitochondrial to nuclear DNA content. Sedentary $Opa1^{+/+}$ ($n = 5$), $Opa1^{+/-}$ ($n = 5$), trained $Opa1^{+/+}$ ($n = 6$), and $Opa1^{+/-}$ ($n = 6$) 8-month-old mice. Values are means \pm SEM. Significant differences: # $P < 0.05$, ## $P < 0.01$ trained versus sedentary, * $P < 0.05$, ** $P < 0.01$ $Opa1^{+/-}$ versus $Opa1^{+/+}$ for sedentary or trained mice.

To understand at which metabolic step FA utilization had been improved, different parameters were measured. HADHA activity, as an index of β -oxidation, was estimated in the four conditions (Fig. 7B), with the results showing a similar profile as for other mitochondrial proteins. Thus, HADHA activity increased more after training in control mice than in *Opa1*^{+/-} mice, with the increases being proportional to CS increase (Fig. 7B, lower panel). We also measured the content of CPT1 and CPT2, the mitochondrial fatty acid transporters (Fig. 7C). Interestingly, while we observed no major difference in CPT1 content in the four groups, we observed a large increase in CPT2 in *Opa1*^{+/-} mice. Normalized to CS content, this increase was still present. This result supports our previous observation of an increase in fatty acid utilization in these animals after training.

Discussion

Mutations in the mitochondrial fusion protein OPA1 are responsible for neurodegeneration of the retinal ganglion cells and induce visual defects. These mutations can also affect respiratory chain complexes and mtDNA content in

skeletal muscle cells (Yu-Wai-Man *et al.* 2010b). It has also been shown that patients with mitochondrial disorders present proteolytic processing of OPA1 that could be involved in the alteration of mitochondria function (Duvezin-Caubet *et al.* 2006). Finally, it is well recognized that exercise training-induced mitochondrial biogenesis causes an increase in fusion and fission protein content (Garnier *et al.* 2005; Iqbal *et al.* 2013). However, the impact of endurance exercise training on mitochondrial biogenesis in patients and in animals with OPA1 mutation is not known. We report here that OPA1 haploinsufficiency in mice did not alter running and training capacity, but greatly improved endurance capacity after training. Adaptation to training in OPA1-deficient mice led to a unique response involving a metabolic shift towards higher FA utilization, probably due to impaired mitochondrial biogenesis.

OPA1 deficiency, exercise capacity and adaptation to exercise training

The OPA1 mutations that are responsible for optic atrophy are present in the whole body and may thus be responsible

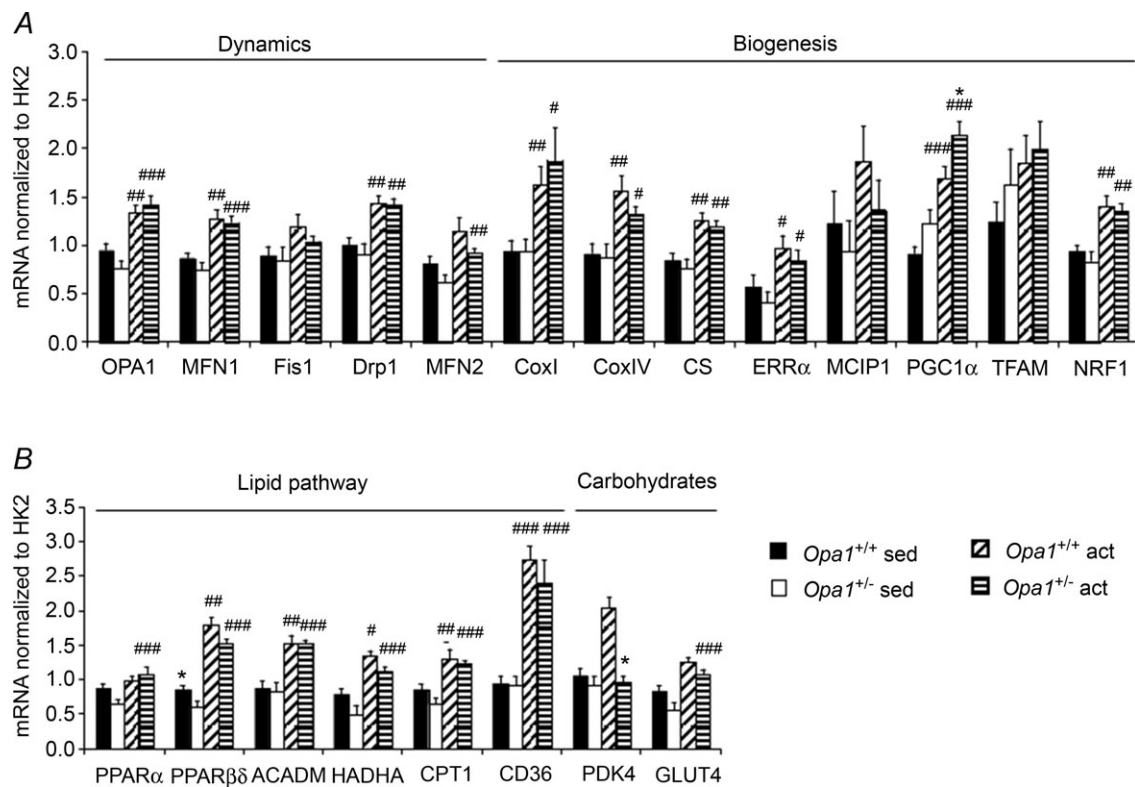


Figure 5. Increased mitochondrial biogenesis in white gastrocnemius muscle
 A and B, mRNA expression levels of proteins. A, proteins involved in mitochondrial dynamics and biogenesis. B, proteins in glucose and lipid utilization pathways. mRNA levels were normalized to mRNA level of HK2. Values are means \pm SEM. Significant differences: *.# $P < 0.05$, **.# $P < 0.01$, ***.### $P < 0.001$. * = *Opa1*^{+/-} versus *Opa1*^{+/+}, # = active versus sedentary. 6-month-old, 2-month trained.

for the cardiac and skeletal muscle alterations. They may also affect exercise capacity. Indeed, heterozygous OPA1 mutations in *Drosophila* cause a reduced escape response, suggesting abnormal function of the skeletal

muscles under stress conditions (Shahrestani *et al.* 2009). This also suggests that patients bearing OPA1 mutations may have altered exercise capacity. Indeed, in patients with dominant optic atrophy, a deficit of oxidative

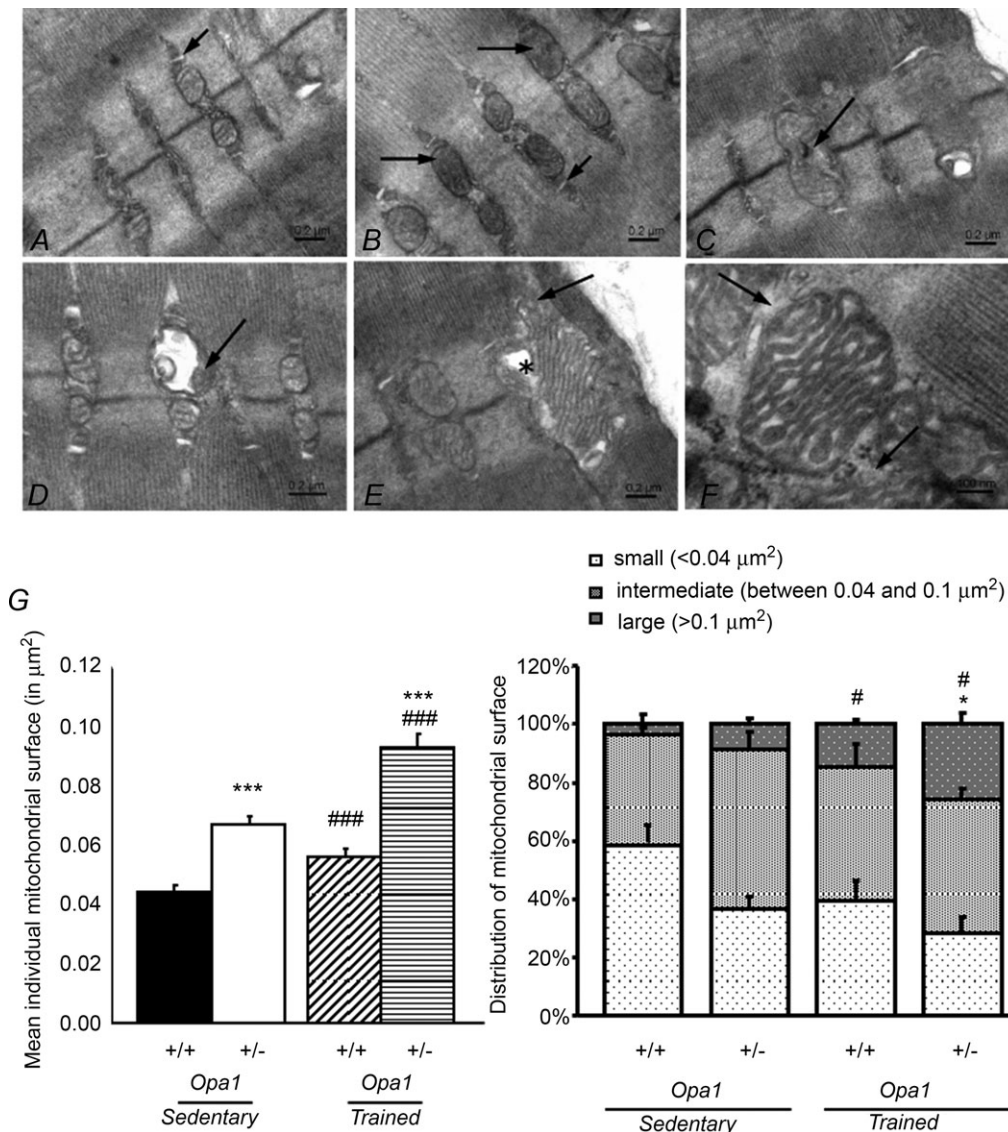


Figure 6. Altered ultrastructure of trained *Opa1*^{+/-} white gastrocnemius muscle

A, control mice. Skeletal muscle shows normal mitochondria with abundant cristae, there is absence of ultrastructural changes inside mitochondria. Mitochondria are placed in their para-Z-disc distribution between the myofibrils, small arrow – triad. B–F, *Opa1*^{+/-} mice. B, the electron micrograph shows slightly dilated mitochondria, some mitochondria deprived of cristae (arrows); small arrow – triad. C, a slightly dilated mitochondrion with regression of cristae and signs of mitochondrial destruction (arrow). D, a vesicular swollen mitochondrion with remnants of matrix compartment (arrow). E, a giant subsarcolemmal mitochondrion showing fragmentation and disappearance of cristae (arrow). The loss of matrix in the mitochondrion is accompanied by the presence of irregular vacuoles (*). F, high magnification of mitochondria with remodelled morphology of cristae, and evidence of disrupted outer mitochondrial membrane (arrows). G, quantification of individual mitochondrial surface in *Opa1*^{+/+} and *Opa1*^{+/-} mice before and after training by analysis of EM white gastrocnemius tissue images. Left panel, average of individual mitochondrial surface estimated on 18 slices per animal (5 different animals for trained and 2 for sedentary animals). Right panel, distribution of individual mitochondrial surface between small (<0.04 μm^2), intermediate (between 0.04 and 0.1 μm^2) or large (>0.1 μm^2) mitochondria. Values are means \pm SEM. Significant differences: *.#*P* < 0.05, ***,###*P* < 0.001. * = *Opa1*^{+/-} versus *Opa1*^{+/+}, # = active versus sedentary.

Table 3. Biochemical parameters

	Sedentary		Trained		Genotype	Training	Interaction
	<i>Opa1</i> ^{+/+}	<i>Opa1</i> ^{+/-}	<i>Opa1</i> ^{+/+}	<i>Opa1</i> ^{+/-}			
Ventricle							
AK	2283 ± 84	2086 ± 75	2489 ± 281	1798 ± 87*	\$	n.s.	n.s.
CK	2546 ± 163	2434 ± 156	2851 ± 300	2276 ± 101	n.s.	n.s.	n.s.
LDH	1408 ± 40	1408 ± 73	1549 ± 160	1284 ± 49	n.s.	n.s.	n.s.
Soleus							
AK	3269 ± 138	3507 ± 184	3353 ± 156	3074 ± 111	n.s.	n.s.	n.s.
CK	5251 ± 241	5192 ± 301	5275 ± 327	4911 ± 131	n.s.	n.s.	n.s.
LDH	1089 ± 60	1145 ± 49	931 ± 62	902 ± 41*	n.s.	\$\$	n.s.
Plantaris							
AK	4612 ± 176	4992 ± 298	5149 ± 188	5039 ± 203	n.s.	n.s.	n.s.
CK	11397 ± 639	12741 ± 372	11632 ± 280	11442 ± 629	n.s.	n.s.	n.s.
mi-CK	166 ± 18	255 ± 53	414 ± 34 ^{##}	386 ± 33 [#]	n.s.	\$\$\$	n.s.
MM-CK	11172 ± 636	12402 ± 329	11265 ± 284	10875 ± 705	n.s.	n.s.	n.s.
MB-CK	59 ± 8	84 ± 14	86 ± 9	93 ± 13	n.s.	n.s.	n.s.
LDH	2373 ± 73	2533 ± 173	2379 ± 89	2148 ± 94	n.s.	n.s.	n.s.
White gastrocnemius							
AK	4861 ± 298	5946 ± 389	5682 ± 287	4959 ± 327	n.s.	n.s.	\$\$
CK	15129 ± 653	16055 ± 1016	15961 ± 800	13692 ± 718	n.s.	n.s.	n.s.
mi-CK	118 ± 25	103 ± 33	150 ± 33	146 ± 21	n.s.	n.s.	n.s.
MM-CK	14937 ± 641	15882 ± 1002	15717 ± 775	13455 ± 720	n.s.	n.s.	n.s.
MB-CK	74 ± 12	70 ± 10	95 ± 13	91 ± 8	n.s.	n.s.	n.s.
LDH	2697 ± 123	3219 ± 292	3217 ± 154	2664 ± 175	n.s.	n.s.	\$

Sedentary *Opa1*^{+/+} (n = 8), *Opa1*^{+/-} (n = 6); trained *Opa1*^{+/+} (n = 9), *Opa1*^{+/-} (n = 9) mice. AK, adenylate kinase; CK, creatine kinase; mi-CK, MM-CK and MB-CK isoforms of CK; LDH, lactate dehydrogenase. Values are means ± SEM (IU (g protein)⁻¹). Significantly different: *^{##}\$ P < 0.05, ^{\$\$}P < 0.01, ^{###}\$\$\$P < 0.001. * = *Opa1*^{+/-} versus *Opa1*^{+/+}, # = active versus sedentary, \$ = global effect of genotype or training.

Table 4. Respiration parameters

	Sedentary		Trained		Genotype	Training	Interaction
	<i>Opa1</i> ^{+/+}	<i>Opa1</i> ^{+/-}	<i>Opa1</i> ^{+/+}	<i>Opa1</i> ^{+/-}			
Plantaris							
V ₀	0.9 ± 0.2	0.5 ± 0.1	1.8 ± 0.3 [#]	1.1 ± 0.1*	\$	\$\$	ns
V _{max}	22.5 ± 2.2	18.9 ± 1.4	24.8 ± 1.8	27.6 ± 3.2 [#]	ns	\$	ns
V FA	2.2 ± 0.2	1.7 ± 0.1	1.8 ± 0.2	3.7 ± 0.8 ^{***##}	ns	\$	\$\$
V Pyr	12.9 ± 2.0	8.5 ± 1.5	11.2 ± 1.5	12.7 ± 1.3	ns	ns	\$
White gastrocnemius							
V ₀	0.6 ± 0.1	0.6 ± 0.1	0.5 ± 0.1	0.5 ± 0.0	ns	ns	ns
V _{max}	15.0 ± 0.8	13.7 ± 0.8	15.7 ± 0.6	14.5 ± 0.6	ns	ns	ns
V FA	0.9 ± 0.1	0.9 ± 0.2	1.0 ± 0.1	1.4 ± 0.1 ^{*##}	ns	\$\$	ns
V Pyr	8.0 ± 0.9	8.3 ± 0.4	7.3 ± 0.8	6.9 ± 0.6	ns	ns	ns

Plantaris: sedentary *Opa1*^{+/+} (n = 7), *Opa1*^{+/-} (n = 7); trained *Opa1*^{+/+} (n = 7), *Opa1*^{+/-} (n = 6) mice. White gastrocnemius: sedentary *Opa1*^{+/+} (n = 9), *Opa1*^{+/-} (n = 9); trained *Opa1*^{+/+} (n = 17), *Opa1*^{+/-} (n = 13) mice. V values are means ± SEM (μmol O₂ min⁻¹ (g dry wt)⁻¹) V₀, respiration rate in malate and ADP. V_{max}, maximal respiration rate in FA, pyruvate, glutamate and succinate. V FA, respiration rate in presence of carnitine and palmitoyl-CoA. V Pyr, respiration rate in pyruvate. Significant differences: *^{##}\$P < 0.05, ^{\$\$}P < 0.01, ^{###}\$\$\$P < 0.001. * = *Opa1*^{+/-} versus *Opa1*^{+/+}, # = active versus sedentary, \$ = global effect of genotype or training.

phosphorylation was evidenced by a decreased rate of post-exercise phosphocreatine resynthesis (Lodi *et al.* 2004, 2011). However, skeletal muscle mitochondrial mass and properties vary greatly with exercise capacity

(Garnier *et al.* 2005) rendering human data sometimes difficult to interpret. We thus studied the exercise and training capacity of sedentary and trained *Opa1*^{+/-} mice by voluntary wheel running and forced exercise on a

treadmill. Because OPA1 deficiency may induce neurological disorders, we first took care to examine the mouse behaviour and found no major impact of the deficiency on anxiety, emotional reactivity, stress-related behaviours or agility, in line with previous studies (Alavi *et al.* 2009). We then examined the exercise capacity of untrained mice

and found that work or running distance did not differ between control and deficient mice. Among the factors that can influence exercise capacity, mouse weight can play a role. We found a slightly lower body weight of *Opa1*^{+/-} mice. We then tested the training ability of the mice. The 8 week running programme led to a significant

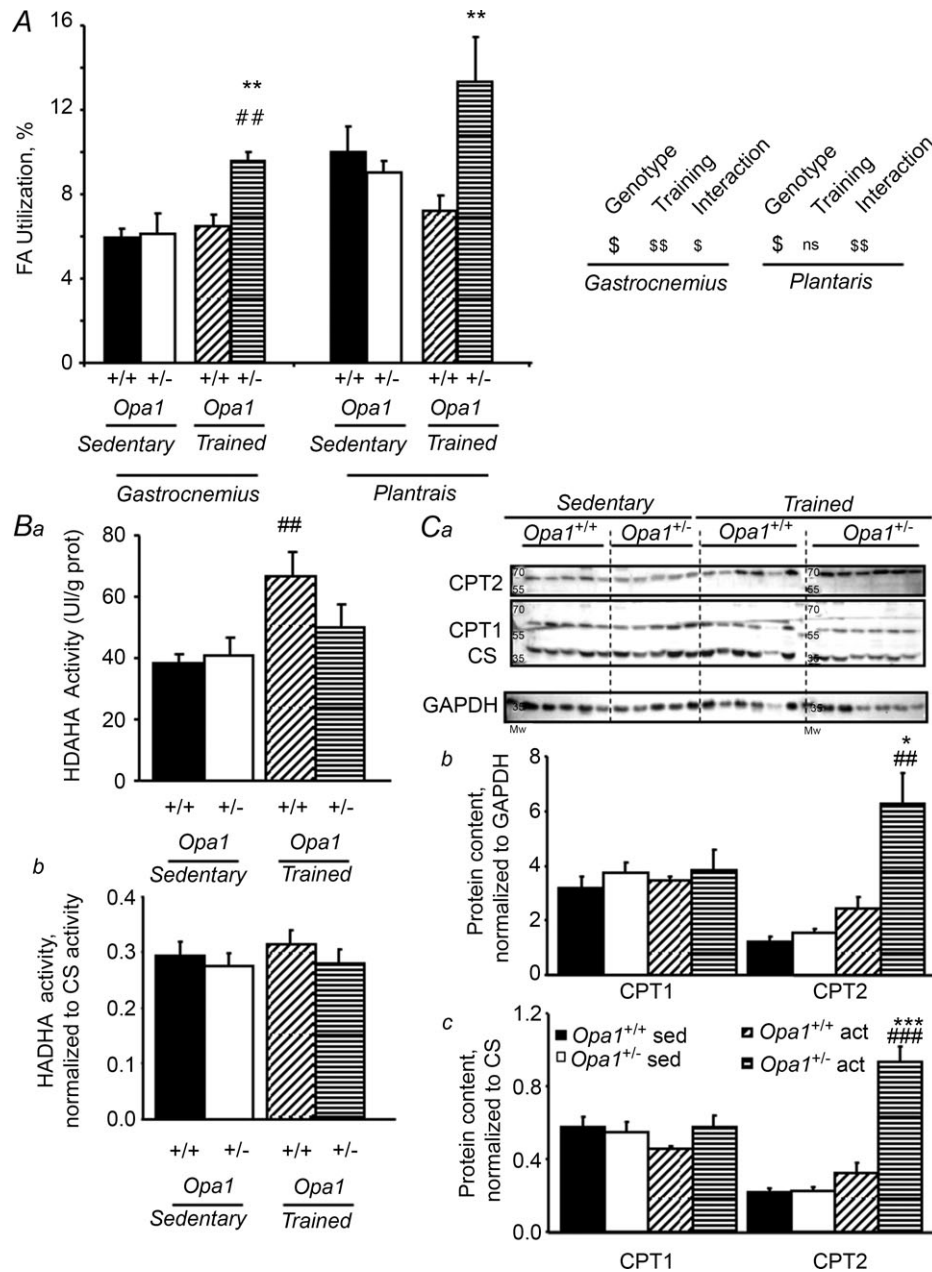


Figure 7. Increased fatty acid oxidation rates in trained fast skeletal muscles of *Opa1*^{+/-} mice

A, respiration rates were measured in saponin-permeabilized fibres of white gastrocnemius and plantaris muscles. Fatty acid utilization rate with carnitine and palmitoyl-CoA is expressed relative to maximal respiration rate with FA, pyruvate, glutamate and succinate. Ba, β -hydroxyacyl-CoA dehydrogenase (HADHA) activity measured spectrophotometrically in white gastrocnemius (GAS) muscles of sedentary and trained mice; Bb, same measurement, normalized to CS activity. Ca, original recording of CPT2 and CPT1 protein content. CS and GAPDH content were used for normalization. Quantification of CPT1 and CPT2, normalized to GAPDH (Cb) or CS (Cc). Values are means \pm SEM. Significantly different: * $P < 0.05$. **.,## $P < 0.01$. **.,### $P < 0.001$. * = *Opa1*^{+/-} versus *Opa1*^{+/+}, # = trained versus sedentary.

improvement in the performance of mice, which again did not differ between strains. This suggests that exercise and training capacities were not altered by OPA1 deficiency. After training, heart weight increased only in *Opa1*^{+/-} mice, providing evidence that training induced a more severe cardiac stress in these mice compensated by an increased cardiac weight, as observed in response to a pathological stress (Piquereau *et al.* 2012).

Endurance exercise performances are mainly dependent on energy metabolism and mitochondrial biogenesis. However, voluntary wheel running represents a moderate type of exercise training. To estimate the maximal endurance exercise abilities of the mice, we performed a forced treadmill running-to-exhaustion test before and after training. To compare the endurance abilities, we carefully matched the maximal aerobic running performance at which the animals ran on the treadmill. Again, in sedentary animals, there was no difference in MAS or running time. However, surprisingly, while training induced a similar increase in MAS of both strains, a striking difference was observed in the time to exhaustion, which was increased more than two-fold in *Opa1*^{+/-} mice, suggesting a unique adaptive strategy.

OPA1 deficiency, exercise training and mitochondrial biogenesis

Currently, only a few studies of mitochondrial dynamics have been conducted on adult differentiated tissues and in response to environmental stress. It has been recognized for a long time that skeletal muscle responds to endurance exercise with an increase in the capacity for aerobic metabolism. This includes increases in both mass and volume of mitochondria, increased enzymes involved in fatty acid metabolism, of the citric acid cycle, and the components of the respiratory chain (Holloszy, 1975). Exercise training is thus one of the main inducers of mitochondrial biogenesis in skeletal muscle. Remodelling of the mitochondrial network plays a central role in the plasticity of skeletal muscle in response to training (Garnier *et al.* 2005; Bo *et al.* 2010). More specifically, endurance training induces an adaptation in the skeletal muscle that requires the coordination of multiple cellular events, with the most dramatic changes occurring at the level of mitochondrial biogenesis. Mitochondrial biogenesis involves not only transcription and translation of mitochondrial proteins, but also a morphological remodelling involving the fusion–fission machinery for separation of daughter mitochondria, and mitochondria affecting correct positioning between myofilaments, under the sarcolemma or around the nucleus. Thus, proper and complete mitochondrial biogenesis requires the coordination and precise succession of molecular and morphological processes.

Starting from the transcriptional machinery, the peroxisome-proliferator activated receptor gamma coactivator-1 α (PGC-1 α) plays a key role in the control of energy metabolism, mitochondrial biogenesis, oxidative muscle fibre switch and angiogenesis (Wu *et al.* 1999; Lin *et al.* 2002; Arany *et al.* 2008). It induces the transcription and co-activates a number of transcription factors involved in mitochondrial biogenesis, like the nuclear respiratory factors (NRFs) and the oestrogen-related receptors (ERRs), and in fatty acid oxidation, such as the peroxisome proliferator-activated receptors (PPARs). Mitochondrial biogenesis was similarly induced in white gastrocnemius muscle of wild-type and *Opa1*^{+/-} mice, as evidenced by increased mRNA expression of transcriptional regulators, mitochondrial proteins and fatty acid oxidation enzymes in fast skeletal muscles. This was also the case for proteins involved in mitochondrial dynamics, although with no major impact on the genotype. This evidence accords with the proposal that proteins involved in mitochondrial dynamics are under the control of the mitochondrial biogenesis programme, and are therefore mainly controlled by PGC-1 α and its transcription cascade and thus similarly respond to exercise training (Garnier *et al.* 2005; Cartoni *et al.* 2005; Bo *et al.* 2010). Importantly, this shows that the signalling pathways involved in the up-regulation of metabolic genes in response to exercise training were similarly activated in both strains and that OPA1 deficiency did not impact on mitochondrial adaptations at the transcription level. This is in accordance with the similar exercise work performed by the mice over the 8 week experimental period (26.0 ± 3.0 kJoules for WT ($n = 21$) versus 30.7 ± 3.5 kJoules ($n = 20$) for *Opa1*^{+/-} mice).

OPA1 has been involved in mtDNA maintenance in skeletal muscle (Amati-Bonneau *et al.* 2008; Elachouri *et al.* 2011). We showed that in *Opa1*^{+/-} mice, fast skeletal muscle mtDNA content was slightly lower than in *Opa1*^{+/+} mice. mtDNA content increased in control mice after training but not in *Opa1*^{+/-} mice. On the other hand, neither COX activity nor expression of the mtDNA encoded COX subunit (COXI) was altered in sedentary animals, suggesting that the small decrease in mtDNA content was not sufficient to affect mitochondrial protein expression.

At the level of mitochondrial enzymes, exercise training induced a more than 50% increase in CS and COX activities in fast but not in slow muscles, but the effects were different in the two mouse strains. Indeed, CS and COX activities, as well as respiratory chain complexes, CS and OPA1 protein content increased less in fast muscles of *Opa1*^{+/-} mice despite a similar increase in mRNA levels, suggesting a defective mitochondrial biogenesis process a step beyond transcription, or an alteration in the mitochondrial protein import process. Because OPA1 plays an important role in the fusion–fission

mechanisms that are involved in the morphological remodelling of mitochondria during biogenesis, a defect in this process may lead to altered mitochondrial structure and mitochondrial protein degradation.

Surprisingly initially, electron microscopic examination of the fast skeletal muscle revealed mitochondria with irregular sizes, especially after training, and a significant increase in mean mitochondrial size in *Opa1*^{+/-} mice which was exacerbated after training. This observation is reminiscent of cardiac cells, in which OPA1 deficiency also led to the accumulation of larger mitochondria with multiple inner membranes (Piquereau *et al.* 2012). It is also consistent with other studies showing that while Mfn2 knock-out mice exhibit mitochondrial fragmentation in neonatal cardiomyocytes, the opposite result, i.e. larger mitochondria, was observed in adult myocardium (Papanicolaou *et al.* 2011). It was thus proposed that, in the constrained environment of striated muscle, a deficit in OPA1 caused by impairing fusion of inner mitochondrial membranes, would compromise further fission mechanisms. Some mitochondria were devoid of cristae and matrix and this was accompanied by formation of irregular vacuoles, suggesting mitochondrial damage. It has already been shown that OPA1-null cells have severe ultrastructural defects in the mitochondria, including swollen mitochondria and defects in cristae organization, such as concentric inner membranes, which were attributed to the role of OPA1 in cristae maintenance (Olichon *et al.* 2003; Song *et al.* 2009; Agier *et al.* 2012). Thus, OPA1 deficiency could impair the normal process of mitochondrial fission during biogenesis and induce defective mitochondria leading to the release of mitochondrial proteins and their degradation. Therefore, for adequate mitochondrial biogenesis to occur, both correct activation of signalling pathways at transcriptional level and optimal remodelling of mitochondria are required. A deficiency of mitochondrial dynamics proteins such as OPA1 can alter mitochondrial morphological remodelling and lead to incomplete mitochondrial biogenesis.

OPA1 deficiency, exercise performance and metabolic remodelling

Surprisingly, mice lacking OPA1 had increased endurance performances after training, despite defective mitochondrial biogenesis. During exercise, muscle contraction induces an increase in ATP requirement. Carbohydrates and lipids are the primary substrates oxidized to generate the ATP required to sustain muscle contraction. It has long been recognized that endurance capacity depends on mitochondrial content as well as on the use of fatty acids, which provide a high quantity of energy for moderate exercise intensity over prolonged

period of time (Holloszy, 1975). While training did not induce an increase in maximal oxidative capacity in the presence of pyruvate and fatty acids in *Opa1*^{+/+}, maximal respiration was significantly increased in *Opa1*^{+/-} mice. This was mainly due to an increase in the capacity of fast skeletal muscle to oxidize fatty acids. Long chain fatty acid oxidation capacity depends on fatty acid delivery to the muscle and on mitochondrial capacity for their transport and oxidation. This involves both transcriptional and post-translational regulations (for review see Holloway *et al.* 2008). It was recently shown that alteration of fatty acid transport in CD36 knock-out mice is sufficient to decrease the endurance time of mice independently of mitochondrial biogenesis and mitochondrial content (McFarlan *et al.* 2012). Conversely, we found an increased endurance time in *Opa1*^{+/-} mice that coincided with increased mitochondrial fatty acid utilization, and increased CD36 expression. Interestingly, there was an increase in CPT2, a fatty acid transport protein of the inner mitochondrial membrane, but not in CPT1, a transport protein of the outer membrane, in trained *Opa1*^{+/-} mice compared to trained *Opa1*^{+/+} mice ($P < 0.001$). This suggests a possible link between OPA1 and CPT2 in the inner mitochondrial membrane. However, adaptation in other metabolic steps and acute regulation of FA utilization could also affect the increased endurance capacity of *Opa1*^{+/-} mice. Measurement of increased fatty acid utilization in fast skeletal muscle of *Opa1* mutants at rest or during exercise should be further explored to gain more insight into adaptive changes in *Opa1*^{+/-} trained fast skeletal muscle.

In conclusion, OPA1 deficiency is not sufficient by itself to alter exercise capacity in mice. OPA1 appears to be important for mitochondrial biogenesis, especially during endurance training. Impairment of mitochondrial biogenesis in *Opa1*^{+/-} mice was compensated by the indirect activation of an adaptive pathway leading to better utilization of the fatty acids affecting increasing endurance performance. Such remodelling does not appear to be deleterious in physiological situations, but could be detrimental in situations of disease states or increased workload.

References

- Adhihetty PJ, Irrcher I, Joseph AM, Ljubicic V & Hood DA (2003). Plasticity of skeletal muscle mitochondria in response to contractile activity. *Exp Physiol* **88**, 99–107.
- Agier V, Oliviero P, Laine J, L'Hermitte-Stead C, Girard S, Fillaut S, Jardel C, Bouillaud F, Bulteau AL & Lombes A (2012). Defective mitochondrial fusion, altered respiratory function, and distorted cristae structure in skin fibroblasts with heterozygous OPA1 mutations. *Biochim Biophys Acta* **1822**, 1570–1580.

- Alavi MV, Bette S, Schimpf S, Schuettauf F, Schraermeyer U, Wehrl HF, Ruttiger L, Beck SC, Tonagel F, Pichler BJ, Knipper M, Peters T, Laufs J & Wissinger B (2007). A splice site mutation in the murine *Opa1* gene features pathology of autosomal dominant optic atrophy. *Brain* **130**, 1029–1042.
- Alavi MV, Fuhrmann N, Nguyen HP, Yu-Wai-Man P, Heiduschka P, Chinnery PF & Wissinger B (2009). Subtle neurological and metabolic abnormalities in an *Opa1* mouse model of autosomal dominant optic atrophy. *Exp Neurol* **220**, 404–409.
- Amati-Bonneau P, Valentino ML, Reynier P, Gallardo ME, Bornstein B, Boissiere A, Campos Y, Rivera H, de la Aleja JG, Carroccia R, Iommarini L, Labauge P, Figarella-Branger D, Marcorelles P, Furby A, Beauvais K, Letournel F, Liguori R, La Morgia C, Montagna P, Liguori M, Zanna C, Rugolo M, Cossarizza A, Wissinger B, Verny C, Schwarzenbacher R, Martin MA, Arenas J, Ayuso C, Garesse R, Lenaers G, Bonneau D & Carelli V (2008). OPA1 mutations induce mitochondrial DNA instability and optic atrophy 'plus' phenotypes. *Brain* **131**, 338–351.
- Arany Z, Foo SY, Ma Y, Ruas JL, Bommi-Reddy A, Girnun G, Cooper M, Laznik D, Chinsomboon J, Rangwala SM, Baek KH, Rosenzweig A & Spiegelman BM (2008). HIF-independent regulation of VEGF and angiogenesis by the transcriptional coactivator PGC-1 α . *Nature* **451**, 1008–1012.
- Bo H, Zhang Y, & Ji LL (2010). Redefining the role of mitochondria in exercise: a dynamic remodeling. *Ann N Y Acad Sci* **1201**, 121–128.
- Cartoni R, Léger B, Hock MB, Praz M, Crettenand A, Pich S, Ziltener JL, Luthi F, Dériaz O, Zorzano A, Gobelet C, Kralli A & Russell AP (2005). Mitofusins 1/2 and ERR α expression are increased in human skeletal muscle after physical exercise. *J Physiol* **567**, 349–358.
- Chan DC (2006). Mitochondria: dynamic organelles in disease, aging, and development. *Cell* **125**, 1241–1252.
- Chen H & Chan DC (2005). Emerging functions of mammalian mitochondrial fusion and fission. *Hum Mol Genet* **14**, R283–R289.
- Chen H, Chomyn A & Chan DC (2005). Disruption of fusion results in mitochondrial heterogeneity and dysfunction. *J Biol Chem* **280**, 26185–26192.
- David DJ, Samuels BA, Rainer Q, Wang JW, Marsteller D, Mendez I, Drew M, Craig DA, Guiard BP, Guilloux JP, Artymyshyn RP, Gardier AM, Gerald C, Antonijevic IA, Leonardo ED & Hen R (2009). Neurogenesis-dependent and -independent effects of fluoxetine in an animal model of anxiety/depression. *Neuron* **62**, 479–493.
- Dimmock D, Tang LY, Schmitt ES & Wong LJ (2010). Quantitative evaluation of the mitochondrial DNA depletion syndrome. *Clin Chem* **56**, 1119–1127.
- Dulawa SC, Holick KA, Gundersen B & Hen R (2004). Effects of chronic fluoxetine in animal models of anxiety and depression. *Neuropsychopharmacology* **29**, 1321–1330.
- Duvezin-Caubet S, Jagasia R, Wagener J, Hofmann S, Trifunovic A, Hansson A, Chomyn A, Bauer MF, Attardi G, Larsson NG, Neupert W & Reichert AS (2006). Proteolytic processing of OPA1 links mitochondrial dysfunction to alterations in mitochondrial morphology. *J Biol Chem* **281**, 37972–37979.
- Elachouri G, Vidoni S, Zanna C, Pattyn A, Boukhaddaoui H, Gaget K, Yu-Wai-Man P, Gasparre G, Sarzi E, Delettre C, Olichon A, Loiseau D, Reynier P, Chinnery PF, Rotig A, Carelli V, Hamel CP, Rugolo M & Lenaers G (2011). OPA1 links human mitochondrial genome maintenance to mtDNA replication and distribution. *Genome Res* **21**, 12–20.
- Frezza C, Cipolat S, Martins de Brito O, Micaroni M, Beznoussenko GV, Rudka T, Bartoli D, Polishuck RS, Danial NN, De Strooper B & Scorrano L (2006). OPA1 controls apoptotic cristae remodeling independently from mitochondrial fusion. *Cell* **126**, 177–189.
- Garnier A, Fortin D, Zoll J, N'Guessan B, Mettauer B, Lampert E, Veksler V & Ventura-Clapier R (2005). Coordinated changes in mitochondrial function and biogenesis in healthy and diseased human skeletal muscle. *FASEB J* **19**, 43–52.
- Habouzit E, Richard H, Sanchez H, Koulmann N, Serrurier B, Monnet R, Ventura-Clapier R & Bigard X (2009). Decreased muscle ACE activity enhances functional response to endurance training in rats, without change in muscle oxidative capacity or contractile phenotype. *J Appl Physiol* **107**, 346–353.
- Holloszy JO (1975). Adaptation of skeletal muscle to endurance exercise. *Med Sci Sports* **7**, 155–164.
- Holloway GP, Luiken JJ, Glatz JF, Spriet LL & Bonen A (2008). Contribution of FAT/CD36 to the regulation of skeletal muscle fatty acid oxidation: an overview. *Acta Physiol (Oxf)* **194**, 293–309.
- Hudson G, Amati-Bonneau P, Blakely EL, Stewart JD, He L, Schaefer AM, Griffiths PG, Ahlqvist K, Suomalainen A, Reynier P, McFarland R, Turnbull DM, Chinnery PF & Taylor RW (2008). Mutation of OPA1 causes dominant optic atrophy with external ophthalmoplegia, ataxia, deafness and multiple mitochondrial DNA deletions: a novel disorder of mtDNA maintenance. *Brain* **131**, 329–337.
- Iqbal S, Ostojic O, Singh K, Joseph AM & Hood DA (2013). Expression of mitochondrial fission and fusion regulatory proteins in skeletal muscle during chronic use and disuse. *Muscle Nerve* DOI: 10.1002/mus.23838.
- Kuznetsov AV, Veksler V, Gellerich FN, Saks V, Margreiter R & Kunz WS (2008). Analysis of mitochondrial function *in situ* in permeabilized muscle fibers, tissues and cells. *Nat Protoc* **3**, 965–976.
- Lin J, Wu H, Tarr PT, Zhang CY, Wu Z, Boss O, Michael LF, Puigserver P, Isotani E, Olson EN, Lowell BB, Bassel-Duby R & Spiegelman BM (2002). Transcriptional co-activator PGC-1 α drives the formation of slow-twitch muscle fibres. *Nature* **418**, 797–801.
- Lira A, Zhou M, Castanon N, Ansoorge MS, Gordon JA, Francis JH, Bradley-Moore M, Lira J, Underwood MD, Arango V, Kung HF, Hofer MA, Hen R & Gingrich JA (2003). Altered depression-related behaviors and functional changes in the dorsal raphe nucleus of serotonin transporter-deficient mice. *Biol Psychiatry* **54**, 960–971.
- Lodi R, Tonon C, Valentino ML, Iotti S, Clementi V, Malucelli E, Barboni P, Longanesi L, Schimpf S, Wissinger B, Baruzzi A, Barbiroli B & Carelli V (2004). Deficit of *in vivo* mitochondrial ATP production in OPA1-related dominant optic atrophy. *Ann Neurol* **56**, 719–723.

- Lodi R, Tonon C, Valentino ML, Manners D, Testa C, Malucelli E, La Morgia C, Barboni P, Carbonelli M, Schimpf S, Wissinger B, Zeviani M, Baruzzi A, Liguori R, Barbiroli B & Carelli V (2011). Defective mitochondrial adenosine triphosphate production in skeletal muscle from patients with dominant optic atrophy due to OPA1 mutations. *Arch Neurol* **68**, 67–73.
- McFarlan JT, Yoshida Y, Jain SS, Han XX, Snook LA, Lally J, Smith BK, Glatz JF, Luiken JJ, Sayer RA, Tupling AR, Chabowski A, Holloway GP & Bonen A (2012). *In vivo*, fatty acid translocase (CD36) critically regulates skeletal muscle fuel selection, exercise performance, and training-induced adaptation of fatty acid oxidation. *J Biol Chem* **287**, 23502–23516.
- Mayorga AJ, Dalvi A, Page ME, Zimov-Levinson S, Hen R & Lucki I (2001). Antidepressant-like behavioral effects in 5-hydroxytryptamine_{1A} and 5-hydroxytryptamine_{1B} receptor mutant mice. *J Pharmacol Exp Ther* **298**, 1101–1107.
- Minasyan A, Keisala T, Zou J, Zhang Y, Toppila E, Syvala H, Lou YR, Kalueff AV, Pyykko I & Tuohimaa P (2009). Vestibular dysfunction in vitamin D receptor mutant mice. *J Steroid Biochem Mol Biol* **114**, 161–166.
- Momken I, Lechene P, Koulmann N, Fortin D, Mateo P, Doan BT, Hoerter J, Bigard X, Veksler V & Ventura-Clapier R (2005). Impaired voluntary running capacity of creatine kinase-deficient mice. *J Physiol* **565**, 951–964.
- Momken I, Lechene P, Ventura-Clapier R & Veksler V (2004). Voluntary physical activity alterations in endothelial nitric oxide synthase knockout mice. *Am J Physiol Heart Circ Physiol* **287**, H914–H920.
- Novotova M, Pavlovicova M, Veksler V, Ventura-Clapier R & Zahradnik I (2006). Ultrastructural remodeling of fast skeletal muscle fibers induced by invalidation of creatine kinase. *Am J Physiol Cell Physiol* **291**, C1279–C1285.
- Olichon A, Baricault L, Gas N, Guillou E, Valette A, Belenguer P & Lenaers G (2003). Loss of OPA1 perturbs the mitochondrial inner membrane structure and integrity, leading to cytochrome c release and apoptosis. *J Biol Chem* **278**, 7743–7746.
- Olichon A, Emorine LJ, Descoins E, Pelloquin L, Brichese L, Gas N, Guillou E, Delettre C, Valette A, Hamel CP, Ducommun B, Lenaers G & Belenguer P (2002). The human dynamin-related protein OPA1 is anchored to the mitochondrial inner membrane facing the inter-membrane space. *FEBS Lett* **523**, 171–176.
- Olichon A, Guillou E, Delettre C, Landes T, Arnaune-Pelloquin L, Emorine LJ, Mils V, Daloyau M, Hamel C, Amati-Bonneau P, Bonneau D, Reynier P, Lenaers G & Belenguer P (2006). Mitochondrial dynamics and disease, OPA1. *Biochim Biophys Acta* **1763**, 500–509.
- Olichon A, Landes T, Arnaune-Pelloquin L, Emorine LJ, Mils V, Guichet A, Delettre C, Hamel C, Amati-Bonneau P, Bonneau D, Reynier P, Lenaers G & Belenguer P (2007). Effects of OPA1 mutations on mitochondrial morphology and apoptosis: relevance to ADOA pathogenesis. *J Cell Physiol* **211**, 423–430.
- Papanicolaou KN, Khairallah RJ, Ngoh GA, Chikando A, Luptak I, O'Shea KM, Riley DD, Lugus JJ, Colucci WS, Lederer WJ, Stanley WC & Walsh K (2011). Mitofusin-2 maintains mitochondrial structure and contributes to stress-induced permeability transition in cardiac myocytes. *Mol Cell Biol* **31**, 1309–1328.
- Piquereau J, Caffin F, Novotova M, Prola A, Garnier A, Mateo P, Fortin D, Huynh le H, Nicolas V, Alavi MV, Brenner C, Ventura-Clapier R, Veksler V & Joubert F (2012). Down-regulation of OPA1 alters mouse mitochondrial morphology, PTP function, and cardiac adaptation to pressure overload. *Cardiovasc Res* **94**, 408–417.
- Piquereau J, Novotova M, Fortin D, Garnier A, Ventura-Clapier R, Veksler V & Joubert F (2010). Postnatal development of mouse heart: formation of energetic microdomains. *J Physiol* **588**, 2443–2454.
- Ramboz S, Oosting R, Amara DA, Kung HF, Blier P, Mendelsohn M, Mann JJ, Brunner D & Hen R (1998). Serotonin receptor 1A knockout: an animal model of anxiety-related disorder. *Proc Natl Acad Sci U S A* **95**, 14476–14481.
- Shahrestani P, Leung HT, Le PK, Pak WL, Tse S, Ocorr K & Huang T (2009). Heterozygous mutation of Drosophila Opa1 causes the development of multiple organ abnormalities in an age-dependent and organ-specific manner. *PLoS One* **4**, e6867.
- Song Z, Ghochani M, McCaffery JM, Frey TG & Chan DC (2009). Mitofusins and OPA1 mediate sequential steps in mitochondrial membrane fusion. *Mol Biol Cell* **20**, 3525–3532.
- Stemmelin J, Cohen C, Terranova JP, Lopez-Grancha M, Pichat P, Bergis O, Decobert M, Santucci V, Francon D, Alonso R, Stahl SM, Keane P, Avenet P, Scatton B, le Fur G & Griebel G (2008). Stimulation of the beta3-Adrenoceptor as a novel treatment strategy for anxiety and depressive disorders. *Neuropsychopharmacology* **33**, 574–587.
- Suen DF, Norris KL & Youle RJ (2008). Mitochondrial dynamics and apoptosis. *Genes Dev* **22**, 1577–1590.
- Ventura-Clapier R, Garnier A & Veksler V (2008). Transcriptional control of mitochondrial biogenesis. The central role of PGC-1 α . *Cardiovasc Res* **79**, 208–217.
- Wu Z, Puigserver P, Andersson U, Zhang C, Adelmant G, Mootha V, Troy A, Cinti S, Lowell B, Scarpulla RC, Spiegelman BM (1999). Mechanisms controlling mitochondrial biogenesis and respiration through the thermogenic coactivator PGC-1. *Cell* **98**, 115–124.
- Yu-Wai-Man P, Griffiths PG, Gorman GS, Lourenco CM, Wright AF, Auer-Grumbach M, Toscano A, Musumeci O, Valentino ML, Caporali L, Lamperti C, Tallaksen CM, Duffey P, Miller J, Whittaker RG, Baker MR, Jackson MJ, Clarke MP, Dhillon B, Czermin B, Stewart JD, Hudson G, Reynier P, Bonneau D, Marques W Jr, Lenaers G, McFarland R, Taylor RW, Turnbull DM, Votruba M, Zeviani M, Carelli V, Bindoff LA, Horvath R, Amati-Bonneau P & Chinnery PF (2010a). Multi-system neurological disease is common in patients with OPA1 mutations. *Brain* **133**, 771–786.

Yu-Wai-Man P, Sitarz KS, Samuels DC, Griffiths PG, Reeve AK, Bindoff LA, Horvath R & Chinnery PF (2010*b*). OPA1 mutations cause cytochrome c oxidase deficiency due to loss of wild-type mtDNA molecules. *Hum Mol Genet* **19**, 3043–3052.

Additional information

Competing interests

None declared.

Author contributions

Conception and design of experiments: F.C., A.P., J.P., M.N., D.D.J., A.G., D.F., R.V.C. and F.J. Collection, analysis and interpretation of data: F.C., A.P., J.P., M.N., D.D.J., A.G., D.F., V.V., R.V.C. and F.J. Drafting the paper and critical revision for important intellectual content: F.C., A.P., J.P., M.N., D.D.J., M.A., V.V., R.V.C. and F.J. All authors have read and approved the final version of the manuscript. Electron microscopy examinations were performed at Institute of Molecular Physiology & Genetics.

Behavior tests, voluntary and forced activities were conducted at IFR 141. All other work was done at INSERM, U-769.

Funding

This work was supported by a PhD grant from Region Ile de France to F.C., a VEGA project 2/0116/12 and APVV SK-FR-0021–11 to M.N., a French/Slovak grant Stefanik 17948XC, and Laboratory of Excellence LERMIT. R.V.C. and F.J. are scientists at the Centre National de la Recherche Scientifique.

Acknowledgements

We thank Dr R. Fischmeister for continuous support. We thank Valérie Domergue-Dupont and the animal core facility of IFR141 for efficient handling and preparation of the animals and Ladislav Novota for the help with electron microscopy studies. We also thank A Lombes for her help with mtDNA quantification. We are grateful to Bernd Wissinger (Genetics Laboratory, Institute for Ophthalmic Research, Centre for Ophthalmology, University of Tübingen, Germany) for sharing the *Opa1*^{+/-} mouse line and to Carina Pripp-Buus (Institut Cochin France) for sharing CPT2 antibody. We finally thank James Wilding for careful reading of the manuscript.